

Running title: Impact of subcellular alterations of organic acids during tomato ripening

Sonia Osorio

Departamento de Biología Molecular y Bioquímica

Universidad de Málaga

29071 Málaga

Spain

Tel: +34 952134268

Fax: +34 952134267

Alteration of the interconversion of pyruvate and malate in the plastid or cytosol of ripening tomato fruit invoke diverse consequences on sugar, yet similar effects on cellular organic acid, metabolism and transitory starch accumulation

Sonia Osorio*, José G. Vallarino, Marek Szecowka, Shai Ufaz, Vered Tzin, Ruthie Angelovici, Gad Galili, Alisdair R. Fernie

Max-Planck-Institut für Molekulare Pflanzenphysiologie, Am Mühlenberg 1, 14476 Potsdam-Golm, Germany (SO, MS and ARF), Departamento de Biología Molecular y Bioquímica, Universidad de Málaga, 29071 Málaga, Spain (SO, JGV), The Weizmann Institute of Science, Rehovot 76100, Israel (SU, VT, RA and GG)

*Corresponding author: Sonia Osorio (Fax: +34952134267, e-mail: sosorio@uma.es)

ABSTRACT

The aim of this work was to investigate the effect of decreased cytosolic phosphoenolpyruvate carboxykinase (PEPCK) and plastidic NADP-dependent malic enzyme (NADP-ME) on tomato (*Solanum lycopersicum*) ripening. Transgenic tomato plants with strongly reduced levels of PEPCK and plastidic NADP-ME were generated by RNA interference gene silencing under the control of a ripening-specific E8 promoter. While these genetic modifications had relatively little effect on the total fruit yield and size, they had strong effects in fruit metabolism. Both transformants were characterized by lower levels of starch at breaker stage. Analysis of the activation state of ADP-glucose pyrophosphorylase correlated with the decrease of starch in both transformants, which suggest that is due to an altered cellular redox status. Moreover, metabolic profiling and feeding experiments involving positional labelled glucoses of fruits lacking in plastidic NADP-malic enzyme and cytosolic PEPCK activities revealed differential changes in overall respiration rates and tricarboxylic acid (TCA) cycle flux. Inactivation of cytosolic PEPCK affected the respiration rate which suggests that excess of oxaloacetate OAA is converted to aspartate and reintroduced in the TCA via 2-oxoglutarate/glutamate. On the other hand, the plastidic NADP-malic enzyme antisense lines were characterized by no changes in respiration rates and TCA cycle flux and together with an increase of pyruvate kinase and phosphoenolpyruvate carboxylase activities indicates that pyruvate is supply through these enzymes to the TCA cycle. These results are discussed in the context of current models of the importance of malate during tomato fruit ripening.

INTRODUCTION

Fruit ripening and development is well established to be under tight genetic control (Matas et al., 2009; Karlova et al., 2011; Klee and Giovannoni, 2011). A growing body of evidence suggests that in parallel large metabolic shifts additionally occur during this process (Carrari and Fernie, 2006; Osorio et al., 2011). Insights into the genetic mechanisms that mediate fruit ripening-related processes, such as cell wall metabolism, pigment synthesis, and sugar metabolism, have resulted from studies that collectively span a wide range of plant species and indicate that they are broadly conserved (Seymour et al., 2008; Moing et al., 2011; Zhang et al., 2011). However, certain species-specific differences exist in the dynamics of other metabolite pools across ripening with for example grape, strawberry, prune and pepper displaying slightly different metabolic programs from tomato (Carrari et al., 2006; Lombardo et al., 2011; Osorio et al., 2011; Osorio et al., 2012; Zamboni et al., 2010; Zhang et al., 2011). This fact notwithstanding, tomato (*Solanum lycopersicum*) has become the primary experimental model in which to study the development and ripening of fleshy fruits (Fernandez et al., 2009; Giovannoni, 2004). It is, furthermore, arguably also the best characterized fruit at the biochemical level (Carrari et al., 2006; Fraser and Bickmore, 2007; Moco et al., 2007; Rose and Bennett, 1999).

One interesting observation is that the levels of several organic acids correlate strongly with transcriptional programs of tomato fruit development (Carrari et al., 2006). This finding led to follow up work demonstrating that the level of malate played an important role in tomato fruit ripening influencing starch accumulation, total soluble solid levels at ripening and post-harvest properties (Centeno et al., 2011), when taken alongside the results of many recent studies on the control of stomatal aperture by malate (Lee et al., 2008; Araujo et al., 2011; Nunes-Nesi et al., 2007; Penfield et al., 2012), thus expanding the documented biological roles for this acid beyond those previously documented (Fernie and

Martinoia, 2009; Meyer et al., 2010). This finding thus suggests that malate metabolism may exert a key influence on the normal ripening and metabolism of tomato fruit. Many of our previous studies were targeted at mitochondrial reactions of the tricarboxylic acid cycle (for reviews see; Sweetlove et al., 2010; Nunes-Nesi et al., 2011), here however, we took RNA interference strategies to silence either the cytosolic PEPCK or the plastidic NADP-dependent malic enzyme (NADP-ME) under the control of the ripening specific E8 promoter. In plants, PEPCK is a cytosolic enzyme which catalyses the ATP-dependent decarboxylation of oxaloacetate (OAA) to phosphoenolpyruvate (PEP) (Chollet et al., 1996). In tomato, PEPCK abundance increases at the start of ripening during which there is a decrease in their malate content (Bahrami et al., 2001). This has led to the suggestion that PEPCK is involved in this dissimilation, and part of this dissimilated malate may be used in gluconeogenesis (Leegood and Walker, 2003; Famiani et al., 2005; Famiani et al., 2009). In contrast, NADP-ME isoforms function in chloroplasts and the cytosol (Drincovich et al., 2001; Gerrard Wheeler et al., 2005), and catalyses the reversible conversion of malate and pyruvate (Farineau and Laval-Martin, 1977; Drincovich et al., 2001). In tomato, NADP-ME has been implicated in respiration during ripening, providing pyruvate and /or NADPH as a substrate for respiration (Farineau and Laval-Martin, 1977; Edwards and Andreo, 1992).

In this study, the two generated lines (*Solanum Lycopersicum* cv MicroTom) with reduced cytosolic *PEPCK* and plastidic *NADP-ME* genes expression were characterized at morphological and biochemical levels including comprehensive metabolite profiling and an evaluation of the effect of these genetic interventions on cellular fluxes. Results are discussed with respect to current models of energy metabolism within the fruit and with respect to the roles of carboxylic acids during fruit ripening and development.

RESULTS

Generation of tomato plants with fruit-specific inhibition of PEPCK and NADP-ME

An 560 bp fragment of the cDNA encoding a cytosolic phosphoenolpyruvate carboxykinase (acc. number AY007226) and a 601 bp fragment of the cDNA encoding a tomato plastidic NADP-malic enzyme1 (acc. number AF001269) were independently cloned using RNAi design, into the pBINplus under the control of the ripening promoter E8. Plants (*Solanum Lycopersicum* cv. Micro-Tom) obtained by an *Agrobacterium tumefaciens* mediated transformation were grown in the greenhouse and seed were collected. Eight lines for RNAi-PEPCK and nine lines for RNAi-ME were selected on the basis of *PEPCK* and *NADP-ME1* gene expression by quantitative real-time PCR (qRT-PCR, Figure 1A and B). Three lines per construct were chosen: PEPCK7, PEPCK10, and PEPCK11 (PEPCK lines) and ME2, ME7, and ME13 (ME lines). Eight T2 plants per line were subsequently grown in the greenhouse and fruits at breaker, breaker + 5 days after pollination (DAP) and breaker + 10 DAP were harvested. Assays of PEPCK and NADP-ME activities revealed that the lines displayed considerable reduction in activity during ripening, respectively, (Tables I and II), and qRT-PCR analysis confirmed that they additionally displayed reduced expression of the *PEPCK* and *NADP-ME1* genes, respectively (Figure 2 A and B). We additionally observed increase in *PEPCK* level during normal tomato ripening while *NADP-ME1* level declined gradually at the onset of ripening as previously have been described (Bahrami 2001; Tomato Genome Consortium 2012) (Figure 2 A and B).

Specific expression of *SINADP-ME* genes

In *Arabidopsis thaliana* genome is known to contain four genes encoding functional NADP-ME isoforms (Gerrard Wheeler et al., 2005). NADP-ME4 is localized to plastids while NADP-ME1, NADP-ME2 and NADP-ME3 are cytosolic isoforms (Gerrard Wheeler et al., 2005; Gerrard Wheeler et al., 2009). The genome of tomato (*Solanum lycopersicum*) possesses three more genes a part of *NADP-ME1* encoding putative NADP-MEs. Cytosolic *NADP-ME2* (AF001270) (Knee and Finger, 1992), plastidic *NADP-ME3* (Solyc03g120990) (Tomato Genome Consortium, 2012), and a putative *NAD(P)-ME4* (Tomato Genome Consortium, 2012). We compared the abundance of all three *NADP-MEs* and *NADP-ME1* transcripts using published tomato (cv. Heinz) RNAseq data from three ripening stages (green, breaker and breaker+10 DAP) (Tomato Genome Consortium, 2012). The expression level of *NADP-ME2* and *NADP-ME1* were similar, while the expression of *NADP-ME3* and *NADP-ME4* accounted for less than 100 times of the *NADP-ME1* and *NADP-ME2* (Tomato Genome Consortium, 2012). Interestingly, *NADP-ME2* and *NADP-ME3* expression were decreasing during ripening while *NADP-ME4* expression was unaltered during fruit ripening (Supplemental Figure 1 and Consortium, 2012). Importantly, qRT-PCR evaluation of the expression level of cytosolic *NADP-ME2*, plastidic *NADP-ME3*, and *NADP-ME4* during ripening in the transgenic ME lines, revealed that the plastidic *NADP-ME3* were decreased in all transgenic lines and in all three ripening stages in comparison to WT (Supplemental Figure 1). However, the levels of the transcripts of *NADP-ME2* and *NADP-ME4* were unaltered in the transformant lines (Supplemental Figure 1).

Fruit size and yield

Fruit size and total fruit yield were determined in fully mature fruit (breaker + 10 DAP). The ME transformants exhibited a significantly lower fruit yield consistent across all three transgenic lines (Figure 1C). Given that fruit size was essentially unaltered (Figure 1D), it is apparent that this was a result of minor decrease in total fruit number in the ME transformants (data not shown). By contrast, PEPCK transformants exhibited unaltered fruit size and yield (Figure 1C and D).

Metabolic profiling of breaker fruits of PEPCK and NADP-ME lines

In order to gain a deeper comprehension of the effects of reducing the expression of these two enzymes we next determined metabolite levels in the pericarp tissue of breaker-stage fruit using an established gas chromatography-mass spectrometry (GC-MS) based metabolite profiling method (Schauer et al., 2006). In the PEPCK lines, we observed a reduction in the levels of the amino acids Asp (all three lines), Ile (lines PEPCK7 and PEPCK11), and Thp (lines PEPCK7 and PEPCK10) (Figure 3). Similarly, a decrease in the levels of citric acid (all three lines), Fru and Glc (all three lines) as well as putrescine (lines PEPCK7 and PEPCK11) was observed (Figure 3). Additionally, PEPCK lines showed an increase in the levels of Glu (all three lines), galactinol (lines PEPCK10 and PEPCK11) (Figure 3). In the ME lines, a smaller number of changes were observed. These lines were characterized by increase of some amino acids, such as Asp (lines ME7 and ME13), Ser (lines ME7 and ME13), Val (lines ME7 and ME13) (Figure 4), sugars and sugar derivatives- such as fucose (lines ME2 and ME7), and *myo*-inositol (lines ME2 and ME13) (Figure 4) as well as putrescine (lines ME2 and ME13).

Metabolic profiling during ripening of PEPCK and NADP-ME fruits

Given that changes in the content of primary metabolites during the ripening process are highly dynamic (Carrari et al., 2006; Fraser et al., 2007; Osorio et al., 2011), we next evaluated metabolite contents during ripening, at breaker + 5 DAP and breaker + 10 DAP stages. In the PEPCK lines, many metabolites at breaker + 5 DAP and breaker + 10 DAP stages displayed similar patterns of change as those observed at breaker stage. This behaviour was observed for amino acids, such as Asp (all three lines), Glu (all three lines), as well as for sugars, such as Fru (all three lines), galactinol (all three lines), Glc (all three lines), fucose (all three lines for breaker + 5 DAP and lines PEPCK7 and PEPCK10 for breaker + 10 DAP), and putrescine (all three lines) (Figure 3). Other changes of note in the metabolites profiles at breaker + 5 DAP stage were the significant increases in dehydroascorbic acid (all three lines), malic acid (all three lines), and rhamnose (all three lines) (Figure 3) as well as decreases in Trp (all three lines), and galacturonic acid (all three lines) (Figure 3). Notably, at breaker + 10 DAP stage, Asn (all three lines), Met (lines PEPCK7 and PEPCK11), Pro (lines PEPCK7 and PEPCK10), GABA (lines PEPCK7 and PEPCK10), and *myo*-inositol (lines PEPCK7 and PEPCK11) were significantly decreased while Tyr was significantly increased (all three lines) (Figure 3). By contrast, evaluation of the primary metabolite composition of ME lines revealed that the pattern of changes in metabolites was more conserved in the comparison between breaker + 5 DAP and breaker + 10 DAP stages than with the breaker stage (Figure 4). Only a reduction in Asp were conserved between the three studied fruit stages. In addition, other conserved changes between breaker + 5 DAP and breaker + 10 DAP stages were noted, such as decreases in the levels of some amino acids, such as GABA, Met, Tyr as well as in the organic acids, galacturonic acid, (Figure 4). Whereas increases of dehydroascorbic acid and rhamnose were observed in the transformants, at these developmental stages (Figure 4).

Deficiency in PEPCK and NADP-ME leads to alteration in nucleotide and starch metabolism

To further characterize these lines, we evaluated one of the major products of the TCA cycle, namely pyrimidine reducing equivalents. This analysis revealed a decrease in NADPH levels in breaker stage of the PEPCK lines (lines PEPCK7 and PEPCK11) but an increase in NAD⁺ (lines PEPCK10 and PEPCK11). Thus, the NADPH/NADP⁺ and NADH/NAD⁺ ratios slightly decreased and increased in PEPCK11, respectively (Table III). By contrast, the pattern of change of pyrimidine levels in the ME lines was markedly different. At breaker stage, the levels of NADP⁺ increased in one line (ME13). As a consequence the NADPH/NADP⁺ ratio decreased (Table IV).

Since pyruvate and PEP metabolites are transformed via the gluconeogenic pathway to sugars-Ps, which can subsequently be converted to starch (Lara et al., 2004) and the fact previous studies demonstrated that phosphoenolpyruvate carboxylase activity (PEPC) plays an important role within potato starch metabolism (Rademacher et al., 2002), we next evaluated starch content of both wild type and transformants at breaker stage (Figure 5). A significant decrease in starch levels was observed in both transgenic sets, PEPCK and ME lines. Therefore, it perhaps suggesting that the rate of transient starch degradation in the fruit is, at least partially, dependent on the total reserves of starch available (Figure 5).

Enzymes involved in starch and organic acid metabolism

To better understand the above-described metabolic alterations we next surveyed the activities of a broad range of enzymes from central metabolism (Table V and VI). In the PEPCK lines, these activities were generally invariant from the wild type, with the exception of the decrease in AGPase and the total NADP-MDH activities in two of the lines (PEPCK7 and PEPCK10) at breaker. In addition, a significant reduction was also observed

in the level (or activity) of pyruvate kinase (PK) in line PEPCK11 and in NAD-malic enzyme and NADP-malic enzyme in line PEPCK7 in the same ripening stage (Table V).

Similar to the situation in the PEPCK lines, analysis of the ME lines at breaker stage revealed that the activities of both AGPase and NADP-MDH decreased in the lines ME2 and ME7 (Table VI). Moreover, a significant increase in PEPC (all three lines) and PK (lines ME2 and ME7) activities was also observed (Table VI).

Respiration in the transgenic fruits

In order to evaluate the effect of deficiencies in the expression of these enzymes on the respiration rate, we next evaluated the relative rate of flux through the major pathways of carbohydrate oxidation at breaker + 5 DAP. For this purpose, we incubated pericarp disks taken from fruits in the light and supplied them with either [1-¹⁴C]-, [3:4-¹⁴C]- or [6-¹⁴C]- Glc for a period of 6 hours. During this period, we collected the ¹⁴CO₂ evolved at hourly intervals. Carbon dioxide can be released from C1 position by the action of enzymes that are not associated with mitochondrial respiration, but carbon dioxide released from the C3,4 positions of glucose cannot (Nunes-Nesi et al., 2005). Thus, the ratio of carbon dioxide evolution from C1 to C3:4 positions of Glc provides an indication of the relative rate of the TCA cycle in comparison to the other routes of carbohydrate oxidation.

When the relative ¹⁴CO₂ release of the transgenic and WT lines was compared an interesting pattern emerges, with a relatively unaltered carbon dioxide evolution in the ME lines but the PEPCK lines displaying considerably altered carbohydrate oxidation. Both lines PEPCK7 and PEPCK10 displayed a greater relative release of ¹⁴CO₂ from C3:4 positions than the WT, indicating a greater flux through the reactions catalysed by pyruvate dehydrogenase and/ or malic enzyme (Figure 6). The difference in release from C6 position was less marked, however, suggesting that there was no alteration in fluxes through pentan synthesis (Stitt and ap Rees, 1979). Despite there being little change in the

absolute release of $^{14}\text{CO}_2$ from the C3,4 in the MADP-malic enzyme lines the relative release from C3,4 positions was considerably higher in line ME2.

Effect of decreased PEPCK and NADP-ME activities on metabolic fluxes

The effect of reduced PEPCK and NADP-ME activities on carbon fluxes was determined by incubating pericarp discs at breaker+10 DAP stage from wild type and two lines of the PEPCK (PEPCK7 and PEPCK10) and ME (ME2 and ME7) transformants with $[\text{U-}^{14}\text{C}]\text{Glc}$ for two hours. Following this incubation the discs were washed and frozen prior by fractionation of the labeled material to determine the label redistribution (Table VII). Neither lines from the PEPCK nor the ME transformants displayed differences from wild type in the total label uptake, or in the metabolized label incorporated into cell wall, amino acids, or sucrose (Table VII). However, there was decreased label incorporation into starch, protein, and organic acids in lines of both transformants (Table VII). Moreover, PEPCK7 and PEPCK10 lines showed a significant decrease of label into the pool of hexoses phosphates (Table VII). Determination of the specific activity of the hexose phosphate pools reveals, as expected that the PEPCK transformants had proportionally lower label in this metabolic pool. On the calculation of the metabolic fluxes it emerged that both transformants, PEPCK and ME, displayed a dramatic decrease in the rate of starch synthesis (Table VII). A similar pattern was found for the fluxes to organic acids and protein, although these changes are considerably less marked than for starch.

Redistribution of ^{13}C label following $[\text{}^{13}\text{C}]\text{-Pyr}$ feeding of transgenic fruits

To further investigate changes in primary metabolism, we fed isotopically labelled $[\text{}^{13}\text{C}]\text{-Pyr}$ to breaker + 10 DAP fruits from PEPCK and ME lines. The absolute redistribution of ^{13}C was measured by assessing the incorporation of the isotope into each intermediate within the relevant pathways (Figure 7) in metabolites closely associated with Pyr using an

adapted GC-MS protocol which facilitates isotope tracing (Roessner-Tunali et al., 2004). Interestingly, the changes in redistribution of isotope were conserved across the transformants.

The PEPCK lines were characterized by elevated label incorporation in fumaric acid, malic acid, and Glu in addition to dramatic elevation in label incorporation in Asp. Moreover, they displayed reduced incorporation in Ala, GABA, Fru, Glc, and succinic acid (Figure 7). However, the pattern of changes in label accumulation in the ME lines was different. That said that were significant increases in label incorporation to citric acid and succinic acid. In contrast decreased label incorporation, in Ala, Glu, fumaric acid, and malic acid was observed (Figure 7).

DISCUSSION

During the ripening of tomato there is a large decrease in the organic acid content of the pericarp (Knee and Finger, 1992; Carrari et al., 2006). This decrease in organic acids could be brought about either by a restriction of their synthesis or an enhanced degradation potentially initially catalysed by either NAD-malic enzyme, NADP-malic enzyme or PEPCK. Malic acid has long implicated in the physiology of fruit ripening (Carrari and Fernie 2006; Sweetman et al., 2009). It has been recently been demonstrated that the level of malic acid plays an important role in regulation of starch biosynthesis and thereby accumulation of total soluble solid during tomato ripening. Detailed biochemical characterisation revealed that this was due to regulation of the activation state of the first committed step of starch synthesis that is catalysed by ADP-glucose pyrophosphorylase (AGPase) (Centeno et al., 2011). Intriguingly, however this is not the first study to implicate reactions beyond the direct pathway of starch biosynthesis since the mitochondrial NAD-malic enzyme (Jenner et al., 2001), the plastidial adenylate kinase (Regierer et al., 2002) and the cytosolic UMP synthase (Geigenberger et al., 2005) have been demonstrated to

be important in determining the levels of starch in storage organs. However, the exact mechanisms of these effects of starch synthesis are essentially unknown although in the case of the adenylate kinase manipulation both the substrate levels and activation status of AGPase reaction were affected (Oliver et al., 2008). In addition, manipulation of malate metabolism in tomato has been demonstrated to effect stomatal opening (Nunes-Nesi et al., 2007; Lee et al., 2008; Araujo et al., 2011; Penfield et al., 2012) and normal root development (van der Merwe et al., 2009). In our previous studies, we focussed on mitochondrial reactions of the TCA cycle and, here, we evaluated the effect of modifying malate:pyruvate balances at different subcellular locations in a fruit ripening-specific manner, by silencing either cytosolic PEPCK or the plastidic NADP-malic enzyme.

Effect of cytosolic PEPCK and plastidic NADP-malic enzyme on starch biosynthesis

Different studies concerning starch metabolism in potato and tomato have suggested that AGPase activity plays an important role in regulation (Geigenberger et al., 1999; Sweetlove et al., 1999; Geigenberger, 2011). AGPase activity is known to be modulate via several different mechanisms. AGPase is sensitive to allosteric regulation, being inhibited by inorganic phosphate and activated by 3PGA (3-phosphoglycerate) (Sowokinos, 1981; Sowokinos and Preiss, 1982). Additionally, it has been demonstrated to be transcriptionally regulated by sugars, nitrate, phosphate and trehalose-6-phosphate (Muller-Rober et al., 1990; Nielsen et al., 1998; Kolbe et al., 2005; Michalska et al., 2009). Moreover, it has been described that AGPase is also redox regulated (Tiessen et al., 2002; Centeno et al., 2011) with malic acid potentially being a key component in this process at least in photosynthetically active tissues (Szecowka et al., 2012).

In tomato, as previously mentioned, a differential regulation of starch biosynthesis was observed in transgenic lines exhibiting different fruit malic acid levels in which the activation stage of AGPase correlated with the accumulation of transitory starch (Centeno

et al., 2011). Similarly, in this context, was the fact that down-regulation of cytosolic PEPCk during ripening resulted in a significant higher malic acid level at the breaker + 5 DAP stage. However, similar down-regulation of the plastidic NADP-malic enzyme during ripening displayed no significant changes in the malic acid level at steady-stage.

The observed decrease in starch content in the cytosolic PEPCk antisense lines at the breaker stage seems to result from an alteration in the malic acid level as previously observed in the TCA cycle transformants (Centeno et al., 2011). However, this correlation was not apparent in plastidic NADP-malic enzyme antisense lines, which also revealed decreased starch content. Interestingly, however, we observed a significant decrease of NADPH in the cytosolic PEPCk lines, which leads to a slightly decrease of NADPH/NADP⁺ ratio. On the other hand, only one line showed changes in the plastidial redox state in the plastidic NADP-malic enzyme antisense lines. Consistent with these changes in the plastidial redox status were the alterations in the activities and activation state of AGPase (in PEPCk and ME lines) and plastidial malate dehydrogenase (in ME lines) which are well documented diagnostics of alteration in redox (Scheible and Stitt, 1988; Tiessen et al., 2002; Nashilevitz et al., 2010). The lack in absolute starch accumulation in both lines was also corroborated with a decrease in the starch biosynthesis flux. Thus the observations described here, demonstrate that as we previously postulated starch metabolism is strongly affected by changes in plastidial redox state but it seems not by altered malate levels *per se*.

When other areas of metabolism are considered some interesting observations are apparent. It is suggested that in fruit ripening, NADP-ME may produce the respiratory substrates pyruvate and NADPH from malate and NADP⁺ (Ruffner, 1982; Drincovich et al., 2001) in cytosol, and maybe thus partake in malate degradation during ripening (Ruffner et al., 1984; Franke and Adams, 1995). Here, feeding experiments involving

incubation of positionally labelled glucoses showed that the strong decrease in plastidic NADP-malic enzyme levels did not lead to substantial changes in overall respiration rates and TCA cycle flux in tomato fruits. Although it is important to note that one line (ME2) was characterized by an increase in the C_{3,4}/C₁ ratio, also suggestive of an increased flux through pyruvate dehydrogenase (albeit one not mediated by an elevated enzymatic capacity of the NAD-malic enzyme). It is conceivable that the remaining activity of plastidic NADP-malic enzyme might still be high enough to supply the TCA cycle with sufficient pyruvate to maintain the overall respiration rate or that there are other alternative sources that may be able to continue to supply the mitochondria with pyruvate or other carbon source, such as cytosolic NADP-ME, pyruvate kinase and phosphoenolpyruvate carboxylase. In the light of this observations it is interesting to note that cytosolic *NADP-ME* expression was not modified in the ME lines. Interestingly, the activities of PK and PEPC enzymes displayed a clear increase in the lines with reduced plastidic NADP-malic enzyme activity. These observations indicate that the lack in plastidic NADP-malic activity made increase the flow through these enzymes, which suggests that plastidic NADP-ME activity is likely an important source of pyruvate synthesis in ripening tomato fruits.

Intriguingly the large decrease in the organic acid content frequently documented as occurring in the pericarp on ripening (Knee and Finger, 1992; Carrari et al., 2006), correlates with a large increase in PEPCK (Bahrami et al., 2001). Thus prompting the question; what is the contribution of this enzyme to flux through the TCA cycle? If the TCA cycle is drained via oxaloacetate (OAA), PEPCK activity requires support neither from PEPC nor PK nor any part of the TCA cycle. However, we can exclude an increase of PK and PEPC activities in compensation to the decrease in cytosolic PEPCK. Moreover, in the PEPCK lines, uniformly labelled glucose feeding experiments also revealed a reduced flux to protein. Furthermore, feeding experiments, involving incubation of positionally

labelled glucoses, suggested that the PEPCK lines displayed higher flux through the reactions catalyzed by either pyruvate dehydrogenase, malic enzyme, or both. This can be concluded from the increased C_{3,4}/C₁ ratios displayed by PEPCK lines since the carbon release from the C_{3,4} position occurs via decarboxylation catalyzed by these enzymes. Both, the mitochondrial NAD- and plastidial NADP-malic enzyme activities showed no differences in the PEPCK lines, which led to suggest that these fruits showed high flux through the TCA cycle via pyruvate dehydrogenase.

PEP required for gluconeogenesis in fruit may originate from malate through the activities of MDH and PEPCK or potentially malic enzymes (Ruffner, 1982). Evidence from radiolabeling work in tomato fruit (Farineau and Laval-Martin, 1977; Halinska and Frenkel, 1991) suggested that gluconeogenesis does occur during ripening stages, when sugars are accumulating rapidly. Here, we observed that when cytosolic PEPCK was reduced (PEPCK lines) led to reduce levels of the major sugars, Glc and Fru during fruit ripening, accompanied by an accumulation of malate which provide further evidence for gluconeogenesis from organic acids (Halinska and Frenkel, 1991) and the important role of PEPCK enzymes in this process.

In order to address the extent to which PEPCK activity contributes to the regulation of the TCA cycle it is first necessary to consider how individual C fluxes around the complete TCA cycle will differ depending on the particular biosynthetic output. When biosynthesis is absent, the net flux of C through each TCA cycle step will be equal, and likewise if the TCA cycle's biosynthetic output is exclusively from oxaloacetate to Asp. By contrast, if the biosynthetic output of the TCA cycle is exclusively from 2-oxoglutarate to Glu, then the flux from malate to 2-oxoglutarate will be proportionately higher than the flux from 2-oxoglutarate to malate. Bearing these considerations in mind, it is interesting that we observed that during ripening the level of Asp derived from OAA, was highly reduced in fruits deficient in PEPCK activity compared to WT. By contrast, the steady-state level of

Glu was higher than in WT during ripening. However, [¹³C] feeding experiment revealed a higher redistribution of the label in both metabolites (Asp, Glu). Interestingly, a higher redistribution of ¹³C label in malic and fumaric acids as well as lower label in succinic acid were also displayed in the PEPCK lines. Although, with these data the flux of C through the TCA cycle from malate to 2-oxoglutarate and from 2-oxoglutarate to malate cannot be calculated, these data indicate that when C in form of OAA cannot be converted into PEP through the activity of PEPCK and thus cannot completely flow through the TCA cycle, the flux from TCA intermediates toward the synthesis of Asp is increased and reintroduced in the TCA via 2-oxoglutarate/Glu.

In conclusion, we present here compelling evidence of the importance of both cytosolic PEPCK and plastidic NADP-malic enzyme in normal tomato ripening metabolism. Both enzymes exhibited a considerable influence on starch biosynthesis metabolism. Their functions in other areas of metabolism are, however, somewhat divergent with our results suggesting that the lack of accumulation of transitory starch was reflected by decrease of major sugars in the PEPCK lines. This observation was not done in plastidic NADP-malic enzyme. Moreover, the inactivation of PEPCK affected the respiration rate suggesting that excess of OAA was converted to Asp and reintroduced in the TCA via 2-oxoglutarate/Glu. These results indicate that the cytosolic PEPCK plays a role in carbon and nitrogen remobilization pathways during fruit ripening. However, further studies will be required to investigate these processes, detailed analysis of starch metabolism revealed that this was impacted by the effect of alterations in the plastid redox status on AGPase. As such these data provide direct support for our earlier model (Centeno et al., 2011) suggesting that malate-mediated effects on starch metabolism are caused by cellular redox changes since the effects on starch, AGPase and pyrimidine nucleotide levels (in PEPCK lines). Rather unexpected, in this context, was the fact that down regulation of plastidic NADP-ME had an effect in starch and AGPase activation state but no effect was observed in malate

levels. This observation demonstrates that changes in plastidial redox state maybe are totally independent of changes in the malate levels. We, also, think that other explanation is that reduction in plastidic NADP-ME activity provokes a small reduction in plastidial malate which was not observed in the global malate pool, but enough to display a change in redox state to affect the activation state of AGPase. Increasing in plastidial malate dehydrogenase corroborated the change in redox state in these plants (Scheible and Stitt, 1988; Tiessen et al., 2002; Nashilevitz et al., 2010).

Additionally, we also found that the negligible impact of reduced NADP-ME activity on respiratory metabolism can be explained by increasing of pyruvate kinase and PEP carboxylase activities, which can compensate the reduction in pyruvate derived from malate via plastidic NADP-ME.

Intriguingly, the changes in redox state observed here are not as severe as those previously described for the TCA cycle manipulations despite the fact that the inhibition of the enzymes modified here is at least as efficient as that in our previous study. For example the lack of apparent changes in pigmentation or post-harvest characteristics indicate that the plastidic NADP-ME and cytosolic PEPCK reactions are quantitatively less important for malate-mediated ripening control than those catalysed by the mitochondrial malate dehydrogenase and fumarase enzymes. There have been recent advances in our understanding of regulation of starch synthesis in response to metabolic signals. However, our knowledge of the signal transduction cascades have not been elucidated but this work highlights the complex interactions that exist between different metabolic pathways and suggests novel approaches for manipulation of starch synthesis.

MATERIAL AND METHODS

Generation of transgenic plants

A 560 bp fragment of *S/PEPCK* (acc. number AY007226) and a 601 bp of *S/NADP-ME* (acc. number AF001269) were independently cloned using the RNAi approach into the vector PBINplus, between the E8 promoter and *ocs* terminator. These constructs were subsequently introduced into plants by *Agrobacterium tumefaciens* mediated transformation protocol. Plants were selected and maintained as described in the literature (Tauberger et al., 2000). Initial screening of eight lines RNAi-PEPCK and 9 lines RNAi-ME were selected on the basis of *PEPCK* and *NADP-ME1* gene expression by qRT-PCR. This screening allowed the identification of three lines per construct that were taken to the next generation.

Analysis of PEPCK and NADP-ME mRNA expression by qRT-PCR

Total RNA was extracted according to Bugos et al. (1995) with minor modifications. Integrity of the extracted RNA was checked by electrophoresis under denaturing conditions after treating the RNA with RNase-free DNaseI (Roche). First-strand cDNA synthesis of 1 mg of RNA in a final volume of 20 mL was performed with Moloney murine leukemia virus reverse transcriptase, Point Mutant RNase H Minus (Promega), according to the supplier's protocol using oligo(dT) T19 primer.

Expression of the cytosolic *PEPCK* and plastidic *NADP-ME* genes was analyzed by real-time qRT-PCR using the fluorescent intercalating dye SYBR Green in an iCycler detection system (Bio-Rad; <http://www.bio-rad.com/>). Relative quantification of the target expression level was performed using the comparative Ct method. The following primers were used: for analysis of *PEPCK* transcript levels (GenBank accession no. AY007226), forward, 5'-AGACGAAACCACTGAGGACGA-3', reverse, 5'-CATTCAACAACACCTTCTCCAA-3'; for *NADP-ME1* (GenBank accession no. AF001269), forward, 5'-CGGTTGAGATGGAGGTTAAATC-3', reverse, 5'-TTACGCAACAATGAGAAACCAC-3'; for *NADP-ME2* (GenBank accession no. AF001270), forward, 5'-TTATTGTTAGTGGTCGCAAGGA-3', reverse, 5'-CGTAAATGTTCTTCCAGTTCCAG-3'; for *NADP-ME3* (GenBank accession no. Solyc03g120990), forward, 5'-CTATGGTGGTGGTCTCTGTGAA-3', reverse, 5'-CTGGAGCATTTTCTTCATCTC-3'; for *NADP-ME4* (GenBank accession no. Solyc08g066290), forward, 5'-AAGAGAACTTGGAGAAGGGATT-3', reverse, 5'-TTATGCGGTTGAGGTAGACGAG-3'.

To normalize gene expression for differences in the efficiency of cDNA synthesis, transcript levels of the constitutively expressed elongation factor 1a of tomato (GenBank accession no. X14449) were measured using the following primers: forward, 5'-ACCACGAAGCTCTCCAGGAG-3', reverse, 5'-CATTGAACCCAACATTGTCACC-3' (Zanor et al., 2009).

Metabolite profiling

Metabolite extraction derivatization, standard addition and sample injection for GC-MS were performed according Schauer et al., (2006). Both chromatograms and mass spectra were evaluated using TAGFINDER (Luedemann et al., 2008). The level of starch in the tissue were determined exactly as described previously (Fernie et al., 2001). NAD⁺, NADP⁺, NADH, and NADPH were determined as previously described (Schippers et al., 2008).

Enzyme assays

NAD-malate dehydrogenase (NAD-MDH), *pyruvate kinase* (PK): The proteins were extracted and assayed as described by Centeno et al. (2011).

AGPase: AGPase activity was measured in the pyrophosphorolysis direction with a spectrophotometric assay, as described Tiessen et al., (2002 and 2003). Frozen tissues were homogenized in liquid N₂ and approx. 100 mg was extracted rapidly (1 min) with 1 ml of extraction buffer (50 mM HEPES-KOH, pH 7.8, and 5 mM MgCl₂) at 4°C. After centrifugation (30 s at 13000g at 4°C), 10 µl of the supernatant was used for the AGPase assay. The reaction was performed in a total volume of 200 µl containing 50 mM HEPES-KOH, pH 7.8, 5 mM MgCl₂, 10 µM Glc-1,6-bisP, 0.6 mM NADP⁺, 2.5 mM Na-PPi, 1 unit/ml phosphoglucomutase, 2.5 units/ml Glc-6-P dehydrogenase, and a range of concentrations of ADP-Glc (0.4-1mM) in the absence of Pi and 3PGA, with or without DTT (10mM) for activation assay. Reactions were followed on line at 340 nm and were linear up to 30 min. The activation state of AGPase is defined as the ratio of V_{sel} (-DTT) to V_{red} (+DTT).

Phosphoenolpyruvate carboxykinase (PEPCK): The protein extraction was performed as is described by Bahrami et al., (2001). The activity of PEPCK was measured in the carboxylation direction, by following oxidation of NADH at 340 nm at room temperature (Walker et al., 1999).

NAD-malic enzyme (NAD-ME) and *Phosphoenolpyruvate carboxylase* (PEPC): The protein extraction and enzyme activity were analysed as described by (Borsani et al., 2009).

NADP-malic enzyme (NADH-ME): 100mg of material was suspended in 100mM Tris-HCl, pH 8.0, 5 mM MgCl₂, 2mM EDTA, 10% (v/v) glycerol and 10 mM 2-mercaptoethanol. The supernatants were collected after centrifugation (10 min at 13000 g). NADP-ME activity was determined at 340nm. The reaction mix contains 50mM Tris-HCl, 10mM MgCl₂, 0.5 nM NADP, and 10 mM malate. The reaction was started by addition of malate (Voll et al., 2012). The optimal pH of the NADP-ME reaction was determined using different buffers for various pH ranges: 100 mM MES pH 5.5, 100 mM Tricine-Mops pH 7.0, 100 mM Tris-HCl pH 7.5, 100 mM Tris-HCl pH 8.0, 100 mM Tris-HCl pH 8.5 as described by Detarsio et al., (2003). We observed that the optimal pH for NADP-ME reaction in tomato fruits was at pH 8.0 (Supplemental Figure 2).

Analysis of [¹³C]-Pyr labelled samples

Disks (10 mm-diameter latitudinal core) from tomato fruits pericarp at breaker + 10 DAP stage from both transgenic lines (PEPCK and ME lines) and WT were fed with 34 mM [¹³C]-Pyr (from Cambridge Isotope Laboratories) by incubation in buffered solution (10 mM MES-KOH, pH 6.5) for a period of 6 h. At the end of the incubation, disks were snap-frozen in liquid nitrogen. They were subsequently extracted in 100% methanol and processed exactly as described by (Timm et al., 2008). The metabolic fate of these substrates was subsequently assessed exactly as described previously (Tieman et al., 2006). A total of four biological replicated were used.

Incubation of plant material with [U-¹⁴C]-Glucose

Disks (10 mm-diameter latitudinal core) from tomato fruits pericarp at breaker + 10 DAP stage from both transgenic lines (PEPCK and ME lines) and WT were taken. Disks were washed three times in fresh incubation medium (10 mM MES-KOH, pH 6.5) and then incubated eight disks in 5 mL of incubation medium containing 1.00 μCi [U-¹⁴C]-Glc (specific activity of 8.11 MBq mmol⁻¹). Samples were then incubated for 2 h before washing again three times in unlabeled incubation medium and freezing in liquid N₂ until further analysis. All incubations were performed in a sealed 100-mL flask at 25°C and shaken at 150 rpm. The evolved ¹⁴CO₂ was collected (in hourly intervals) in 0.5 mL of 10%

(w/v) KOH and the amount of radiolabel was subsequently quantified by liquid scintillation counting. After this step, the disks were harvested, washed three times in buffer (eight disks per 100 mL), and frozen in liquid nitrogen to enable further analysis. A total of four biological replicates were used.

Fractionation of ^{14}C -labeled material

Tissue was fractionated exactly as described by Fernie et al. (2001), with the exception that hexoses were fractionated enzymatically rather than utilizing thin-layer chromatography as described in Carrari et al. (2006). Labeled Suc levels were determined after 4 h of incubation of 200 μL of total neutral fraction with 4 units mL^{-1} hexokinase in 50 mM Tris-HCl, pH 8.0, containing 13.3 mM MgCl_2 and 3.0 mM ATP at 25°C. For labeled Glc and Fru levels, 200 μL of neutral fraction was incubated with 1 unit mL^{-1} Glc oxidase and 32 units mL^{-1} peroxidase in 0.1 M potassium phosphate buffer, pH 6, for a period of 6 h at 25°C. After the incubation time, all reactions were stopped by heating at 95°C for 5 min. The label was separated by ion-exchange chromatography as described by Fernie et al. (2001). The reliability of these fractionation techniques has been thoroughly documented (Runquist and Kruger, 1999; Fernie et al., 2001; Carrari et al., 2006) previously. Fluxes were calculated as described by Fernie et al. (2001), following the assumptions detailed by Geigenberger et al. (1997, 2000).

Acknowledgements

We acknowledge the excellent care of the plants by Helga Kulka (Max-Planck-Institut für Molekulare Pflanzenphysiologie) and Hanna Levanony (Weizmann Institute of Sciences). This work was partially supported by the ERAnet –financed project TomQML (S.O. and A.R.F.).

Supplemental data

The following materials are available in the online version of this article.

Supplemental Figure 1. Expression of *SINADP-ME* genes during tomato ripening.

Supplemental Figure 2. NADP-ME activity of WT tomato at breaker stage in a various pH ranges.

Figure legends

Figure 1. Characterization and expression of tomato cytosolic PEPCK and NADP-ME.

(A, B) Screening by quantitative RTPCR in primary PEPCK and ME transformants in extracts of tissue sampled at breaker + 10 DAP. Black narrow indicate the lines selected for further analysis. (C) Total fruit yield and (D) fruit size of the PEPCK and ME lines. For all parameters, determines values are presented as the mean \pm SE of eight biological replicates (one biological replicate is represented by one individual plant). An asterisk indicates the values that were determined by the *t* test to be significantly different ($P < 0.05$) from wild type.

Figure 2. PEPCK and ME expression during ripening of PEPCK and ME lines.

(A, B) The abundance of *PEPCK* (acc. number AY007226) and *NADPH-ME1* (acc. number AF001269) mRNAs were measured by quantitative RT-PCR, respectively. The ripening stages were as follows: breaker, breaker + 5 DAP, and breaker + 10 DAP. Values are presented as means \pm SE of six individual plants per line. Asterisks indicate significant differences of transgenic lines against the WT for each stage using the ANOVA and Tukey HSD test adjusted to 95% significant level. Different letters indicate significant differences within the WT line in the different ripening stages, using the ANOVA and Tukey HSD test adjusted to 95% significant level.

Figure 3. Primary metabolite levels in the receptacle of WT and PEPCK lines at three ripening stages (B; B+5 DAP; B+10 DAP).

Data are normalized to the mean value of WT at the B stage. Values are means SE of three replicates. Black points indicate significant differences by *t* test ($P < 0.05$) of the transgenic lines compared with WT at the same developmental stage.

Figure 4. Primary metabolite levels in the receptacle of WT and ME lines at three ripening stages (B; B+5 DAP; B+10 DAP).

Data are normalized to the mean value of WT at the B stage. Values are means SE of three replicates. Black points indicate significant differences by *t* test ($P < 0.05$) of the transgenic lines compared with WT at the same developmental stage.

Figure 5. Starch content of PEPCK and ME lines.

(A) Starch content in the PEPCK and (B) ME lines at breaker stage. Values are presented as means \pm SE of six individual plants per line. An asterisk indicates the values that were determined by the *t* test to be significantly different ($P < 0.05$) from wild type.

Figure 6. Respiratory parameters in Breaker + 10 DAP fruits of PEPCK and NADP-ME lines.

(A, B) Evolution of $^{14}\text{CO}_2$ from breaker + 10 DAP pericarp discs of PEPCK and ME lines, respectively. (C, D) Ratio of dioxide evolution from C3,4/C1 positions of glucose in breaker +10 DAP pericarp discs of PEPCK and ME lines, respectively.

Figure 7. Redistribution of ^{13}C label following incubation of transgenic lines (PEPCK and ME) and WT fruits (breaker + 10 DAP stage).

The absolute isotope redistribution (μmol fraction carbon enrichment g^{-1} FW h^{-1}) after incubation period of 6 h of $[\text{U-}^{13}\text{C}]$ Pyr. Values are means \pm SE of determinations on four independent sampling; and asterisk indicates values that were determined by the Student's *t* test to be significantly different ($P < 0.05$) from WT.

Supplemental Figure 1. Expression of *SINADP-MEs* during ripening.

The abundance of *NADP-ME2* (acc. number AF001270), *NADPH-ME3* (acc. number Solyc03g120990), and *NADPH-ME4* (acc. number Solyc08g066290) mRNAs were measured by quantitative RT-PCR, respectively. The ripening stages were as follows: breaker, breaker + 5 DAP, and breaker + 10 DAP. Values are presented as means \pm SE of six individual plants per line. Asterisks indicate significant differences of transgenic lines against the WT for each stage using the ANOVA and Tukey HSD test adjusted to 95% significant level. Different letters indicate significant differences within the WT line in the different ripening stages, using the ANOVA and Tukey HSD test adjusted to 95% significant level.

Supplemental Figure 2. NADP-ME activity of WT tomato at breaker stage in a various pH ranges. Values are presented as the mean \pm SE of 6 biological determinations.

REFERENCES

- Araujo WL, Nunes-Nesi A, Osorio S, Usadel B, Fuentes D, Nagy R, Balbo I, Lehmann M, Studart-Witkowski C, Tohge T, Martinoia E, Jordana X, Damatta FM and Fernie AR** (2011) Antisense inhibition of the iron-sulphur subunit of succinate dehydrogenase enhances photosynthesis and growth in tomato via an organic acid-mediated effect on stomatal aperture. *Plant Cell* **23**(2): 600-627
- Bahrami AR, Chen ZH, Walker RP, Leegood RC and Gray JE** (2001) Ripening-related occurrence of phosphoenolpyruvate carboxykinase in tomato fruit. *Plant Mol. Biol.* **47**(4): 499-506
- Borsani J, Budde CO, Porrini L, Lauxmann MA, Lombardo VA, Murray R, Andreo CS, Drincovich MF and Lara MV** (2009) Carbon metabolism of peach fruit after harvest: changes in enzymes involved in organic acid and sugar level modifications. *J. Exp. Bot.* **60**(6): 1823-1837
- Bugos RC, Chiang VL, Zhang XH, Campbell ER, Podila GK and Campbell WH** (1995) RNA isolation from plant tissues recalcitrant to extraction in guanidine. *Biotechniques* **19**: 734-737
- Carrari F, Baxter C, Usadel B, Urbanczyk-Wochniak E, Zanon MI, Nunes-Nesi A, Nikiforova V, Centro D, Ratzka A, Pauly M, Sweetlove LJ and Fernie AR** (2006) Integrated analysis of metabolite and transcript levels reveals the metabolic shifts that underlie tomato fruit development and highlight regulatory aspects of metabolic network behavior. *Plant Physiol.* **142**(4): 1380-1396
- Carrari F and Fernie AR** (2006) Metabolic regulation underlying tomato fruit development. *J. Exp. Bot.* **57**(9): 1883-1897
- Centeno DC, Osorio S, Nunes-Nesi A, Bertolo AL, Carneiro RT, Araujo WL, Steinhauser MC, Michalska J, Rohrmann J, Geigenberger P, Oliver SN, Stitt M, Carrari F, Rose JK and Fernie AR** (2011) Malate plays a crucial role in starch metabolism, ripening, and soluble solid content of tomato fruit and affects postharvest softening. *Plant Cell* **23**(1): 162-184
- Chollet R, Vidal J and O'Leary MH** (1996) Phosphoenolpyruvate carboxylase: A Ubiquitous, Highly Regulated Enzyme in Plants. *Annu Rev Plant Physiol Plant mol Biol.* **47**: 273-298
- Detarsio E, Gerrard Wheeler MC, Campos-Bermúdez V, Andreo CS and Drincovich MF** (2003) Maize C₄ NADP-Malic Enzyme. *J Biol Chem* **278**(16): 13757-13764
- Drincovich MF, Casati P and Andreo CS** (2001) NADP-malic enzyme from plants: a ubiquitous enzyme involved in different metabolic pathways. *FEBS letters* **490**(1-2): 1-6
- Edwards GE and Andreo CS** (1992) NADP-malic enzyme from plants. *Phytochemistry* **31**(6): 1845-1857

Famiani F, Baldicchi A, Battistelli A, Moscatello S and Walker RP (2009) Soluble sugar and organic acid contents and the occurrence and potential role of phosphoenolpyruvate carboxykinase (PEPCK) in gooseberry (*Ribes grossularia* L.). *J. Hort. Sci. Biotech.* **84**: 249-254

Famiani F, Cultrera NG, Battistelli A, Casulli V, Proietti P, Standardi A, Chen ZH, Leegood RC and Walker RP (2005) Phosphoenolpyruvate carboxykinase and its potential role in the catabolism of organic acids in the flesh of soft fruit during ripening. *J. Exp. Bot.* **56**(421): 2959-2969

Farineau J and Laval-Martin D (1977) Light versus Dark Carbon Metabolism in Cherry Tomato Fruits: II. Relationship Between Malate Metabolism and Photosynthetic Activity. *Plant Physiol.* **60**(6): 877-880

Fernandez AI, Viron N, Alhag Dow M, Karimi M, Jones M, Amsellem Z, Sicard A, Czerednik A, Angenent G, Grierson D, May S, Seymour G, Eshed Y, Lemaire-Chamley M, Rothan C and Hilson P (2009) Flexible tools for gene expression and silencing in tomato. *Plant Physiol.* **151**(4): 1729-1740

Fernie AR, Roscher A, Ratcliffe RG and Kruger NJ (2001) Fructose 2,6-bisphosphate activates pyrophosphate: fructose-6-phosphate 1-phosphotransferase and increases triose phosphate to hexose phosphate cycling in heterotrophic cells. *Planta* **212**(2): 250-263

Fernie AR, Martinoia E (2009) Malate. Jack of all trades or master of a few?. *Phytochemistry* **70**(7): 828-832

Franke KE and Adams DO (1995) Cloning of a full-length cDNA for malic enzyme (EC 1.1.1.40) from grape berries. *Plant Physiol.* **107**(3): 1009-1010

Fraser P and Bickmore W (2007) Nuclear organization of the genome and the potential for gene regulation. *Nature* **447**(7143): 413-417

Fraser PD, Enfissi EM, Halket JM, Truesdale MR, Yu D, Gerrish C and Bramley PM (2007) Manipulation of phytoene levels in tomato fruit: effects on isoprenoids, plastids, and intermediary metabolism. *Plant Cell* **19**(10): 3194-3211

Geigenberger P, Reimholz R, Geiger M, Merlo L, Canale V, Stitt M (1997) Regulation of sucrose and starch metabolism in potato tubers in response to short-term water deficit. *Planta* **201**: 502-518

Geigenberger P, Muller-Rober B and Stitt M (1999) Contribution of adenosine 5'-diphosphoglucose pyrophosphorylase to the control of starch synthesis is decreased by water stress in growing potato tubers. *Planta* **209**(3): 338-345

Geigenberger P, Fernie AR, Gibon Y, Christ M, Stitt M (2000) Metabolic activity decreases as an adaptive response to low internal oxygen in growing potato tubers. *Biol. Chem.* **381**: 723–740

Geigenberger P, Regierer B, Nunes-Nesi A, Leisse A, Urbanczyk-Wochniak E, Springer F, van Dongen JT, Kossmann J and Fernie AR (2005) Inhibition of de novo pyrimidine synthesis in growing potato tubers leads to a compensatory stimulation of the pyrimidine salvage pathway and a subsequent increase in biosynthetic performance. *Plant Cell* **17**(7): 2077-2088

Geigenberger P (2011) Regulation of starch biosynthesis in response to a fluctuating environment. *Plant Physiol.* **155**(4): 1566-1577.

Gerrard Wheeler M, Arias CL, Maurino VG, Andreo CS and Drincovich MF (2009) Identification of domains involved in the allosteric regulation of cytosolic *Arabidopsis thaliana* NADP-malic enzyme. *FEBS letters* **276**: 5665-5677

Gerrard Wheeler MC, Tronconi MA, Drincovich MF, Andreo CS, Flugge UI and Maurino VG (2005) A comprehensive analysis of the NADP-malic enzyme gene family of *Arabidopsis*. *Plant Physiol.* **139**(1): 39-51

Giovannoni JJ (2004) Genetic regulation of fruit development and ripening. *Plant Cell* **16 Suppl**: S170-180

Halinska A and Frenkel C (1991) Acetaldehyde stimulation of net gluconeogenic carbon movement from applied malic Acid in tomato fruit pericarp tissue. *Plant Physiol.* **95**(3): 954-960

Jenner HL, Winning BM, Millar AH, Tomlinson KL, Leaver CJ and Hill SA (2001) NAD malic enzyme and the control of carbohydrate metabolism in potato tubers. *Plant Physiol.* **126**(3): 1139-1149

Karlova R, Rosin FM, Busscher-Lange J, Parapunova V, Do PT, Fernie AR, Fraser PD, Baxter C, Angenent GC and de Maagd RA (2011) Transcriptome and metabolite profiling show that APETALA2a is a major regulator of tomato fruit ripening. *Plant Cell* **23**(3): 923-941

Klee HJ and Giovannoni JJ (2011) Genetics and control of tomato fruit ripening and quality attributes. *Annu. rev. Genet.* **45**: 41-59

Knee M and Finger FL (1992) NADP⁺ malic enzyme and organic acid levels in developing tomato fruits. *J. Am. Soc. Hort. Sci.* **117**: 799-801

Kolbe A, Tiessen A, Schluepmann H, Paul M, Ulrich S and Geigenberger P (2005) Trehalose 6-phosphate regulates starch synthesis via posttranslational redox activation of ADP-glucose pyrophosphorylase. *PNAS* **102**(31): 11118-11123

Lara MV, Drincovich MF and Andreo CS (2004) Induction of a crassulacean acid-like metabolism in the C(4) succulent plant, *Portulaca oleracea* L: study of enzymes involved in carbon fixation and carbohydrate metabolism. *Plant & Cell Physiol.* **45**(5): 618-626

Lee M, Choi Y, Burla B, Kim YY, Jeon B, Maeshima M, Yoo JY, Martinoia E and Lee Y (2008) The ABC transporter AtABCB14 is a malate importer and modulates stomatal response to CO₂. *Nat. Cell Biol.* **10**: 1217-1223

Leegood RC and Walker RP (2003) Regulation and roles of phosphoenolpyruvate carboxykinase in plants. *Arch. Biochem. Biophys.* **414**(2): 204-210

Lombardo VA, Osorio S, Borsani J, Lauxmann MA, Bustamante CA, Budde CO, Andreo CS, Lara MV, Fernie AR, Drincovich MF (2011) Metabolic profiling during peach fruit development and ripening reveals the metabolic networks that underpin each developmental stage. *Plant Physiol* **157**(4): 1696-1710

Luedemann A, Strassburg K, Erban A, Kopka J (2008) Tagfinder for quantitative analysis of gas chromatography-mass spectrometry (GC-MS)-based metabolite profiling experiments. *Bioinformatics* **24**(5):732-737

Matas AJ, Gapper NE, Chung MY, Giovannoni JJ and Rose JK (2009) Biology and genetic engineering of fruit maturation for enhanced quality and shelf-life. *Curr. Opin. Biotech.* **20**(2): 197-203

Meyer S, De Angeli A, Fernie AR, Martinoia E (2010) Intra- and extra-cellular excretion of carboxylates. *Trends Plant Sci* **15**(1): 40-47

Michalska J, Zauber H, Buchanan BB, Cejudo FJ and Geigenberger P (2009) NTRC links built-in thioredoxin to light and sucrose in regulating starch synthesis in chloroplasts and amyloplasts. *PNAS* **106**(24): 9908-9913

Moco S, Capanoglu E, Tikunov Y, Bino RJ, Boyacioglu D, Hall RD, Vervoort J and De Vos RC (2007) Tissue specialization at the metabolite level is perceived during the development of tomato fruit. *J. Exp. Bot.* **58**(15-16): 4131-4146

Moing A, Aharoni A, Biais B, Rogachev I, Meir S, Brodsky L, Allwood JW, Erban A, Dunn WB, Kay L, de Koning S, de Vos RC, Jonker H, Mumm R, Deborde C, Maucourt M, Bernillon S, Gibon Y, Hansen TH, Husted S, Goodacre R, Kopka J, Schjoerring JR, Rolin, D and Hall RD (2011) Extensive metabolic cross-talk in melon fruit revealed by spatial and developmental combinatorial metabolomics. *New Phytol.* **190**(3): 683-696

Muller-Rober BT, Kossmann J, Hannah LC, Willmitzer L and Sonnewald U (1990) One of two different ADP-glucose pyrophosphorylase genes from potato responds strongly to elevated levels of sucrose. *Mol. Gen. Genet.* **224**(1): 136-146

Nashilevitz S, Melamed-Bessudo C, Izkovich Y, Rogachev I, Osorio S, Itkin M, Adato A, Pankratov I, Hirschberg J, Fernie AR, Wolf S, Usadel B, Levy AA, Rumeau D and Aharoni A (2010) An orange ripening mutant links plastid NAD(P)H dehydrogenase complex activity to central and specialized metabolism during tomato fruit maturation. *Plant Cell* **22**(6): 1977-1997

Nielsen TH, Krapp A, Roper-Schwarz U and Stitt M (1998) The sugar-mediated regulation of genes encoding the small subunit of Rubisco and the regulatory subunit of ADP glucose pyrophosphorylase is modified by phosphate and nitrogen. *Plant Cell Environ.* **21**: 443-454

Nunes-Nesi A, Carrari F, Lytovchenko A, Smith AM, Loureiro ME, Ratcliffe RG, Sweetlove LJ and Fernie AR (2005) Enhanced photosynthetic performance and growth as a consequence of decreasing mitochondrial malate dehydrogenase activity in transgenic tomato plants. *Plant Physiol.* **137**(2): 611-622

Nunes-Nesi A, Carrari F, Gibon Y, Sulpice R, Lytovchenko A, Fisahn J, Graham J, Ratcliffe RG, Sweetlove LJ and Fernie AR (2007) Deficiency of mitochondrial fumarate hydratase activity in tomato plants impairs photosynthesis via an effect on stomatal function. *The Plant Journal* **50**(6): 1093-1106

Nunes-Nesi A, Araujo WL and Fernie AR (2011) Targeting mitochondrial metabolism and machinery as a means to enhance photosynthesis. *Plant Physiol.* **155**(1): 101-107

Oliver SN, Tiessen A, Fernie AR and Geigenberger P (2008) Decreased expression of plastidial adenylate kinase in potato tubers results in an enhanced rate of respiration and a stimulation of starch synthesis that is attributable to post-translational redox-activation of ADP-glucose pyrophosphorylase. *J. Exp. Bot.* **59**(2): 315-325

Osorio S, Alba R, Nikoloski Z, Kochevenko A, Fernie AR and Giovannoni JJ (2012) Integrative comparative analyses of transcript and metabolite profiles from pepper and tomato ripening and development stages uncovers species-specific patterns of network regulatory behaviour. *Plant Physiol.* **159**(4): 1713-1729

Osorio S, Alba R, Damasceno CM, Lopez-Casado G, Lohse M, Zanon MI, Tohge T, Usadel B, Rose JK, Fei Z, Giovannoni JJ and Fernie AR (2011) Systems biology of tomato fruit development: combined transcript, protein, and metabolite analysis of tomato transcription factor

(nor, rin) and ethylene receptor (Nr) mutants reveals novel regulatory interactions. *Plant Physiol.* **157**(1): 405-425

Penfield S, Clements S, Bailey KJ, Gilday AD, Leegood RC, Gray JE and Graham IA (2012) Expression and manipulation of phosphoenolpyruvate carboxykinase 1 identifies a role for malate metabolism in stomatal closure. *The Plant Journal* **69**(4): 679-688

Rademacher T, Hausler RE, Hirsch HJ, Zhang L, Lipka V, Weier D, Kreuzaler F and Peterhansel C (2002) An engineered phosphoenolpyruvate carboxylase redirects carbon and nitrogen flow in transgenic potato plants. *The Plant Journal* **32**(1): 25-39

Regierer B, Fernie AR, Springer F, Perez-Melis A, Leisse A, Koehl K, Willmitzer L, Geigenberger P and Kossmann J (2002) Starch content and yield increase as a result of altering adenylate pools in transgenic plants. *Nat Biotechnol.* **20**(12): 1256-1260

Roessner-Tunali U, Liu J, Leisse A, Balbo I, Perez-Melis A, Willmitzer L and Fernie AR (2004) Kinetics of labelling of organic and amino acids in potato tubers by gas chromatography-mass spectrometry following incubation in (¹³C) labelled isotopes. *Plant J.* **39**: 668–679

Rose JK and Bennett AB (1999) Cooperative disassembly of the cellulose-xyloglucan network of plant cell walls: parallels between cell expansion and fruit ripening. *Trends Plant Sci* **4**(5): 176-183

Ruffner HP (1982) Metabolism of tartaric and malic acids in *Vitis*: a review-Part A. *Vitis* **21**: 346-358

Ruffner HP, Possner D, Brem S and Rast DM (1984) The physiological role of malic enzyme in grape ripening. *Planta* **160**: 444-448

Runquist M, Kruger NJ (1999) Control gluconeogenesis by isocitrate lyase in endosperm of germinating castor bean seedlings. *Plant J* **19**(4): 423-431

Scheible R and Stitt M (1988) Comparison of NADP-malate dehydrogenase activation QA reduction and O₂ evolution in spinach leaves. *Plant Physiol Biochem* **26**: 473-481

Schauer N, Semel Y, Roessner U, Gur A, Balbo I, Carrari F, Pleban T, Perez-Melis A, Bruedigam C, Kopka J, Willmitzer L, Zamir D and Fernie AR (2006) Comprehensive metabolic profiling and phenotyping of interspecific introgression lines for tomato improvement. *Nat Biotechnol.* **24**(4): 447-454

Schippers JH, Nunes-Nesi A, Apetrei R, Hille J, Fernie AR and Dijkwel PP (2008) The *Arabidopsis* onset of leaf death5 mutation of quinolinate synthase affects nicotinamide adenine dinucleotide biosynthesis and causes early ageing. *Plant Cell* **20**(10): 2909-2925

- Seymour G, Poole M, Manning K and King GJ** (2008) Genetics and epigenetics of fruit development and ripening. *Curr Opin Plant Biol* **11**(1): 58-63
- Sowokinos JR** (1981) Pyrophosphorylases in *Solanum tuberosum*: II. Catalytic properties and regulation of ADP-glucose and UDP-glucose pyrophosphorylase activities in potatoes. *Plant Physiol.* **68**(4): 924-929
- Sowokinos JR and Preiss J** (1982) Pyrophosphorylases in *Solanum tuberosum*: III. Purification, physical, and catalytic properties of ADP-glucose pyrophosphorylase in potatoes. *Plant Physiol.* **69**(6): 1459-1466
- Stitt M, ap Rees T** (1979) Capacities of pea chloroplasts to catalyse the oxidative pentose phosphate pathway and glycolysis. *Phytochemistry* **18**:1905-1911
- Sweetlove LJ, Beard KFM, Nunes-Nesi A, Fernie AR, Ratcliffe RG** (2010) Not just a circle: flux modes in the plant TCA cycle. *Trends Plant Sci* **15**: 462-470
- Sweetlove LJ, Muller-Rober B, Willmitzer L and Hill SA** (1999) The contribution of adenosine 5'-diphosphoglucose pyrophosphorylase to the control of starch synthesis in potato tubers. *Planta* **209**(3): 330-337
- Sweetman C, Deluc LG, Cramer GR, Ford CM and Soole KL** (2009) Regulation of malate metabolism in grape berry and other developing fruits. *Phytochemistry* **70**(11-12): 1329-1344
- Szeczowka M, Osorio S, Obata T, Araujo W, Rohrmann J, Nunes-Nesi A and Fernie AR** (2012) Decreasing the mitochondrial synthesis of malate in potato tubers does not affect plastidial starch synthesis suggesting that the physiological regulation of ADPglucose pyrophosphorylase is context-dependent. *Plant Physiol.* DOI: 10.1104/pp.112.204826
- Tauberger E, Fernie AR, Emmermann M, Renz A, Kossmann J, Willmitzer L and Trethewey RN** (2000) Antisense inhibition of plastidial phosphoglucomutase provides compelling evidence that potato tuber amyloplasts import carbon from the cytosol in the form of glucose-6-phosphate. *The Plant Journal* **23**(1): 43-53
- Tieman D, Taylor M, Schauer N, Fernie AR, Hanson AD, Klee HJ** (2006) Tomato aromatic amino acid decarboxylases participate in synthesis of the flavor volatiles 2-phenylethanol and 2-phenylacetaldehyde. *PNAS* **103**: 8287–8292
- Tiessen A, Prescha K, Branscheid A, Palacios N, McKibbin R, Halford NG, Geigenberger P** (2003) Evidence that SNF1-related kinase and hexokinase are involved in separate sugar-

signalling pathways modulating post-translational redox activation of ADP-glucose pyrophosphorylase in potato tubers. *Plant J* **35**(4): 490-500

Tiessen A, Hendriks JH, Stitt M, Branscheid A, Gibon Y, Farre EM and Geigenberger P (2002) Starch synthesis in potato tubers is regulated by post-translational redox modification of ADP-glucose pyrophosphorylase: a novel regulatory mechanism linking starch synthesis to the sucrose supply. *Plant Cell* **14**(9): 2191-2213

Timm S, Nunes-Nesi A, Parnik T, Morgenthal K, Wienkoop S, Keerberg O, Weckwerth W, Kleczkowski LA, Fernie AR and Bauwe H (2008) A cytosolic pathway for the conversion of hydroxypyruvate to glycerate during photorespiration in *Arabidopsis*. *Plant Cell* **20**(10): 2848-2859

Tomato Genome Consortium (2012) The tomato genome sequence provides insights into fleshy fruit evolution. *Nature* **485**(7400): 635-641

van der Merwe MJ, Osorio S, Moritz T, Nunes-Nesi A and Fernie AR (2009) Decreased mitochondrial activities of malate dehydrogenase and fumarase in tomato lead to altered root growth and architecture via diverse mechanisms. *Plant Physiol.* **149**(2): 653-669

Voll LM, Zell MB, Engelsdorf T, Saur A, Wheeler MG, Drincovich MF, Weber AP and Maurino VG (2012) Loss of cytosolic NADP-malic enzyme 2 in *Arabidopsis thaliana* is associated with enhanced susceptibility to *Colletotrichum higginsianum*. *New Phytol.* **195**(1): 189-202

Walker RP, Chen ZH, Tecsi LI, Famiani F, Lea PJ and Leegood RC (1999) Phosphoenolpyruvate carboxykinase plays a role in interactions of carbon and nitrogen metabolism during grape seed development. *Planta* **210**(1): 9-18

Zamboni A, Di Carli M, Guzzo F, Stocchero M, Zenoni S, Ferrarini A, Tononi P, Toffali K, Desiderio A, Lilley KS, Pe ME, Benvenuto E, Delledonne M, Pezzotti M (2010) Identification of putative stage-specific grapevine berry biomarkers and omics data integration into networks. *Plant Physiol* **154**(3): 1439-1459

Zanor MI, Osorio S, Nunes-Nesi A, Carrari F, Lohse M, Usadel B, Kuhn C, Bleiss W, Giavalisco P, Willmitzer L, Sulpice R, Zhou YH and Fernie AR (2009) RNA interference of LIN5 in tomato confirms its role in controlling Brix content, uncovers the influence of sugars on the levels of fruit hormones, and demonstrates the importance of sucrose cleavage for normal fruit development and fertility. *Plant Physiol.* **150**(3): 1204-1218

Zhang J, Wang X, Yu O, Tang J, Gu X, Wan X and Fang C (2011) Metabolic profiling of strawberry (*Fragaria x ananassa* Duch.) during fruit development and maturation. *J. Exp. Bot.* **62**(3): 1103-1118

Table I. PEPCK activity during tomato fruit ripening of PEPCK lines. Values are presented as the mean \pm SE of 6 biological determinations. The values that are significantly different by t test from the wild type are set in bold type ($P < 0.05$).

	Breaker	Breaker + 5 DAP	Breaker + 10 DAP
PEPCK activity ($\mu\text{mol}/\text{min g FW}$)			
WT	0.027 \pm 0.003	0.045 \pm 0.003	0.036 \pm 0.003
PEPCK7	0.020 \pm 0.001	0.035 \pm 0.004	0.030 \pm 0.002
PEPCK10	0.018 \pm 0.002	0.033 \pm 0.004	0.028 \pm 0.004
PEPCK11	0.015 \pm 0.002	0.037 \pm 0.005	0.032 \pm 0.003

Table II. NADP-ME activity during tomato fruit ripening of ME lines. Values are presented as the mean \pm SE of 6 biological determinations. The values that are significantly different by t test from the wild type are set in bold type ($P < 0.05$).

	Breaker	Breaker + 5 DAP	Breaker + 10 DAP
NADP-ME ($\mu\text{mol}/\text{min g FW}$)			
WT	1.23 \pm 0.08	0.75 \pm 0.04	0.66 \pm 0.07
ME2	0.77 \pm 0.09	0.41 \pm 0.08	0.38 \pm 0.05
ME7	0.65 \pm 0.05	0.37 \pm 0.06	0.35 \pm 0.04
ME13	0.70 \pm 0.07	0.39 \pm 0.07	0.37 \pm 0.07

Table III. Pyridine nucleotide levels in breaker fruits in PEPCK antisense lines. Values are presented as the mean \pm SE of 6 biological determinations. The values that are significantly different by t test from the wild type are set in bold type ($P < 0.05$).

	WT		PEPCK7		PEPCK10		PEPCK11	
	Breaker (nmol/g FW)							
NADPH	43.32	\pm 1.73	33.05	\pm 0.94	40.93	\pm 1.10	31.62	\pm 1.43
NADP ⁺	10.37	\pm 0.84	8.34	\pm 0.34	9.76	\pm 1.02	10.34	\pm 0.74
NADP(H)	53.69	\pm 2.81	41.39	\pm 1.1	50.69	\pm 2.18	41.96	\pm 2.2
NADPH/NADP ⁺	4.18	\pm 0.51	3.96	\pm 0.27	4.19	\pm 0.55	3.06	\pm 0.36
NADH	74.27	\pm 2.45	71.37	\pm 1.67	78.22	\pm 3.02	75.2	\pm 2.89
NAD ⁺	33.47	\pm 1.39	29.48	\pm 2.04	37.48	\pm 1.34	28.77	\pm 0.94
NAD(H)	107.74	\pm 5.58	100.85	\pm 5.49	115.7	\pm 6.61	103.97	\pm 4.90
NADH/NAD ⁺	2.22	\pm 0.17	2.42	\pm 0.22	2.09	\pm 0.16	2.61	\pm 0.19

Table IV. Pyridine nucleotide levels in breaker fruits in ME antisense lines. Values are presented as the mean \pm SE of 6 biological determinations. The values that are significantly different by t test from the wild type are set in bold type ($P < 0.05$).

	WT		ME2		ME7		ME13	
	Breaker (nmol/g FW)							
NADPH	43.32	\pm 1.73	40.48	\pm 0.83	41.38	\pm 1.34	44.27	\pm 1.44
NADP ⁺	10.37	\pm 0.84	9.36	\pm 0.57	12.36	\pm 1.48	15.37	\pm 1.23
NADP(H)	53.69	\pm 2.81	49.84	\pm 1.21	53.74	\pm 3.44	59.64	\pm 3.14
NADPH/NADP ⁺	4.18	\pm 0.51	4.32	\pm 0.35	3.35	\pm 0.51	2.88	\pm 0.32
NADH	74.27	\pm 2.45	75.27	\pm 1.45	72.45	\pm 1.72	73.11	\pm 0.95
NAD ⁺	33.47	\pm 1.39	35.40	\pm 0.93	31.23	\pm 1.10	33.13	\pm 0.86
NAD(H)	107.74	\pm 5.58	110.67	\pm 2.57	103.68	\pm 3.37	106.24	\pm 1.73
NADH/NAD ⁺	2.22	\pm 0.17	2.13	\pm 0.10	2.32	\pm 0.14	2.21	\pm 0.09

Table V. Enzymatic activities in breaker fruits in the PEPCK Lines. Values are presented as the mean \pm SE of 6 biological determinations. The values that are significantly different by t test from the wild type are set in bold type ($P < 0.05$).

Enzymatic activities	WT		PEPCK7		Breaker				PEPCK11	
AGPase (+PGA) (nmol/min g FW)	15.67	\pm 1.37	11.23	\pm 1.20	10.98	\pm 0.98			13.34	\pm 1.17
AGPase (-PGA) (nmol/min g FW)	11.37	\pm 1.02	9.34	\pm 0.89	8.99	\pm 0.94			10.37	\pm 0.85
AGPase activation state (Vsel/Vred)	0.82	\pm 0.04	0.71	\pm 0.03	0.73	\pm 0.02			0.73	\pm 0.01
NADP-MDH total (nmol/min g FW)	0.53	\pm 0.07	0.37	\pm 0.03	0.41	\pm 0.02			0.38	\pm 0.07
NADP-MDH inicial (nmol/min g FW)	0.15	\pm 0.04	0.14	\pm 0.07	0.15	\pm 0.05			0.12	\pm 0.06
NADP-MDH activation stage (nmol/min g FW)	0.82	\pm 0.05	0.78	\pm 0.07	0.8	\pm 0.03			0.75	\pm 0.07
NAD-MDH (μ mol/min g FW)	4.52	\pm 0.32	4.33	\pm 0.41	4.83	\pm 0.27			4.99	\pm 0.37
Pyruvate kinase (nmol/min g FW)	0.83	\pm 0.09	0.75	\pm 0.07	0.88	\pm 0.05			0.69	\pm 0.07
Phospho <i>eno</i> lpyruvate carboxylase (μ mol/min g FW)	0.29	\pm 0.06	0.26	\pm 0.04	0.27	\pm 0.07			0.24	\pm 0.03
NAD-malic enzyme (μ mol/min g FW)	0.61	\pm 0.05	0.50	\pm 0.04	0.59	\pm 0.05			0.52	\pm 0.06
NADP-malic enzyme (μ mol/min g FW)	1.23	\pm 0.08	0.87	\pm 0.05	1.15	\pm 0.09			1.26	\pm 0.08

Table VI. Enzymatic activities in breaker fruits in the ME lines. Values are presented as the mean \pm SE of 6 biological determinations. The values that are significantly different by t test from the wild type are set in bold type ($P < 0.05$).

Enzymatic activities	WT			ME2			ME7			ME13		
	Breaker											
AGPase (+PGA) (nmol/min g FW)	15.67	\pm	1.37	12.73	\pm	1.03	11.38	\pm	1.12	16.73	\pm	2.03
AGPase (-PGA) (nmol/min g FW)	11.37	\pm	1.02	8.36	\pm	0.93	7.23	\pm	1.02	12.21	\pm	0.93
AGPase activation state (Vsel/Vred))	0.82	\pm	0.04	0.69	\pm	0.04	0.73	\pm	0.02	0.80	\pm	0.04
NADP-MDH total (nmol/min g FW)	0.53	\pm	0.07	0.37	\pm	0.05	0.38	\pm	0.06	0.56	\pm	0.04
NADP-MDH inicial (nmol/min g FW)	0.15	\pm	0.04	0.11	\pm	0.03	0.18	\pm	0.04	0.18	\pm	0.05
NADP-MDH activation stage (nmol/min g FW)	0.82	\pm	0.05	0.74	\pm	0.04	0.85	\pm	0.05	0.88	\pm	0.05
NAD-MDH (μ mol/min g FW)	4.52	\pm	0.32	4.01	\pm	0.42	4.78	\pm	0.27	3.98	\pm	0.34
Pyruvate kinase (nmol/min g FW)	0.83	\pm	0.09	1.21	\pm	0.09	1.43	\pm	0.08	0.93	\pm	0.07
Phosphoenolpyruvate carboxylase (μ mol/min g FW)	0.29	\pm	0.06	0.42	\pm	0.05	0.37	\pm	0.06	0.40	\pm	0.06
NAD-malic enzyme μ mol/min g FW)	0.61	\pm	0.05	0.68	\pm	0.05	0.58	\pm	0.04	0.55	\pm	0.06
PEPCK (μ mol/min g FW) (x10)	0.36	\pm	0.03	0.42	\pm	0.04	0.39	\pm	0.03	0.32	\pm	0.04

Table VII. Metabolism of [U-¹⁴C]Glc in pericarp disks from PEPCK and ME lines at breaker + 10 DAP fruits. Pericarp disk were cut from growing of six separate plants per genotype. After 2 h of incubation, the disks were extracted and fractionated. The specific activity of the hexose phosphate pool was estimated by dividing the label retained in the phosphate ester pool by the summed carbon of the hexose phosphates, and used to calculate absolute fluxes. Values represent mean ± SE of 6 biological determinations. The values that are significantly different by t test from the wild type are set in bold type ($P < 0.05$).

Parameter	WT	PEPCK7	PEPCK10	ME2	ME7
Label incorporated (Bq)					
Total uptake	287.2 ± 16.5	235.2 ± 12.2	208.3 ± 14.8	260.6 ± 19.2	269.5 ± 5.4
Insoluble					
Starch	10.2 ± 0.2	5.5 ± 0.6	6.3 ± 1.0	4.8 ± 0.6	5.1 ± 0.2
Cell wall	5.1 ± 0.7	5.2 ± 0.5	6.4 ± 1.0	4.1 ± 0.5	6.0 ± 0.7
Protein	3.0 ± 0.3	1.7 ± 0.1	1.4 ± 0.1	0.9 ± 0.1	1.7 ± 0.2
Soluble					
Organic acids	130.7 ± 8.6	96.9 ± 11.3	65.0 ± 3.8	76.7 ± 6.4	86.7 ± 6.6
Total hexoses-P	11.3 ± 2.2	6.1 ± 2.7	6.4 ± 2.1	10.2 ± 3.5	12.3 ± 2.8
Amino acids	104.3 ± 2.2	84.5 ± 7.7	85.4 ± 7.0	125.1 ± 9.0	114.9 ± 16.1
Sucrose	31.1 ± 4.4	27.3 ± 1.1	27.7 ± 2.4	30.8 ± 1.7	31.4 ± 2.7
Specific activity (dpm nmol ⁻¹ g FW ⁻¹)					
Hexose-P pool	19.3 ± 0.8	13.6 ± 0.7	12.9 ± 0.5	19.3 ± 0.5	18.3 ± 0.4
Metabolic flux (nmol ⁻¹ g FW ⁻¹)					
Starch	621.0 ± 94.3	434.2 ± 75.4	376.4 ± 112.3	587.3 ± 84.4	393.0 ± 77.5
Cell wall	84.4 ± 21.3	94.3 ± 17.4	103.3 ± 17.3	91.8 ± 20.3	103.3 ± 19.4
Organic acids	193.4 ± 22.5	134.4 ± 14.4	153.5 ± 15.5	89.5 ± 17.4	149.4 ± 23.5
Amino acids	224.5 ± 17.5	204.4 ± 17.2	194.4 ± 20.4	248.4 ± 16.4	235.4 ± 21.4
Protein	54.4 ± 9.4	39.4 ± 8.4	37.2 ± 10.8	28.4 ± 8.2	68.3 ± 6.4
Sucrose	76.3 ± 7.4	86.3 ± 6.4	79.3 ± 5.6	80.3 ± 9.4	70.4 ± 7.8

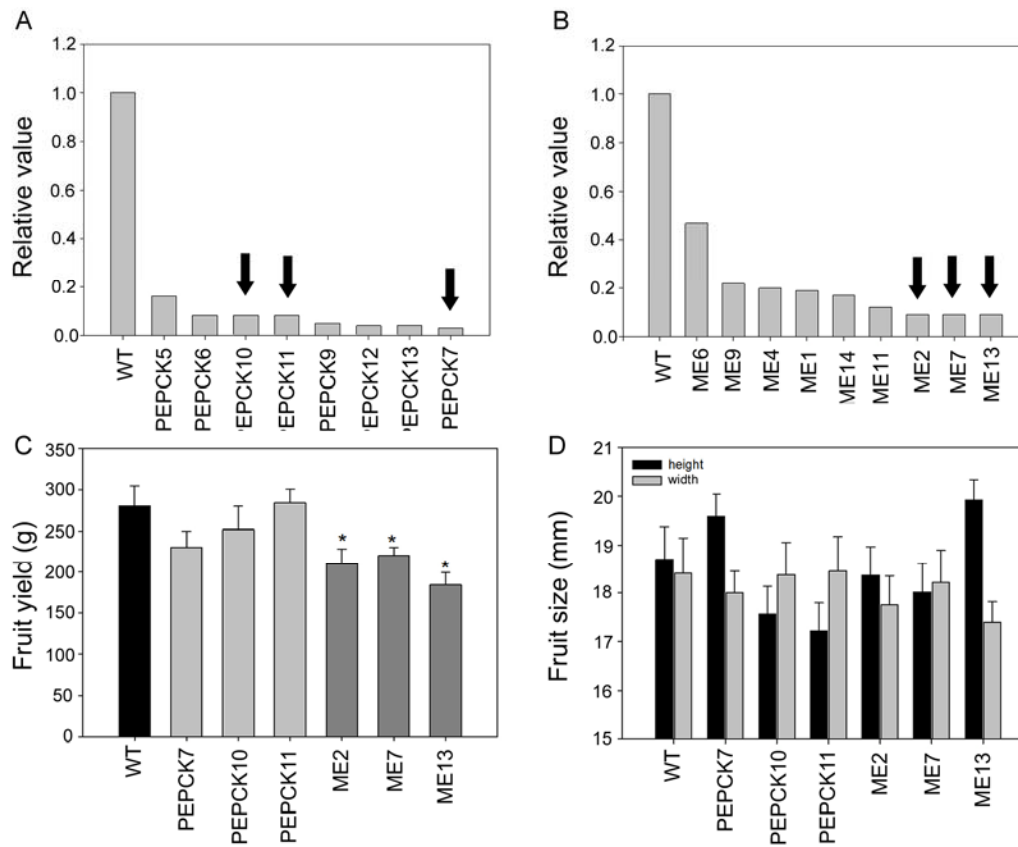


Figure 1. Characterization and expression of tomato cytosolic PEPCK and NADP-ME.

(A, B) Screening by quantitative RTPCR in primary PEPCK and ME transformants in extracts of tissue sampled at breaker + 10 DAP. Black narrow indicate the lines selected for further analysis.

(C) Total fruit yield and (D) fruit size of the PEPCK and ME lines. For all parameters, determines values are presented as the mean \pm SE of eight biological replicates (one biological replicate is represented by one individual plant). An asterisk indicates the values that were determined by the *t* test to be significantly different ($P < 0.05$) from wild type.

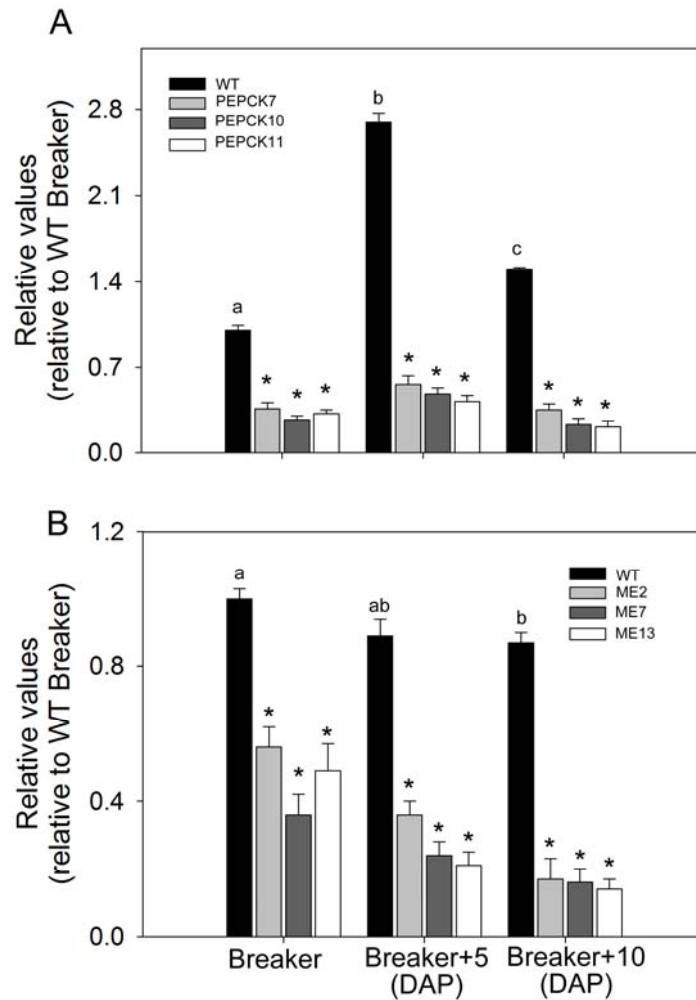


Figure 2. *PEPCK* and *ME* expression during ripening of *PEPCK* and *ME* lines.

(A, B) The abundance of *PEPCK* (acc. number AY007226) and *NADPH-ME1* (acc. number AF001269) mRNAs were measured by quantitative RT-PCR, respectively. The ripening stages were as follows: breaker, breaker + 5 DAP, and breaker + 10 DAP. Values are presented as means \pm SE of six individual plants per line. Asterisks indicate significant differences of transgenic lines against the WT for each stage using the ANOVA and Tukey HSD test adjusted to 95% significant level. Different letters indicate significant differences within the WT line in the different ripening stages, using the ANOVA and Tukey HSD test adjusted to 95% significant level.

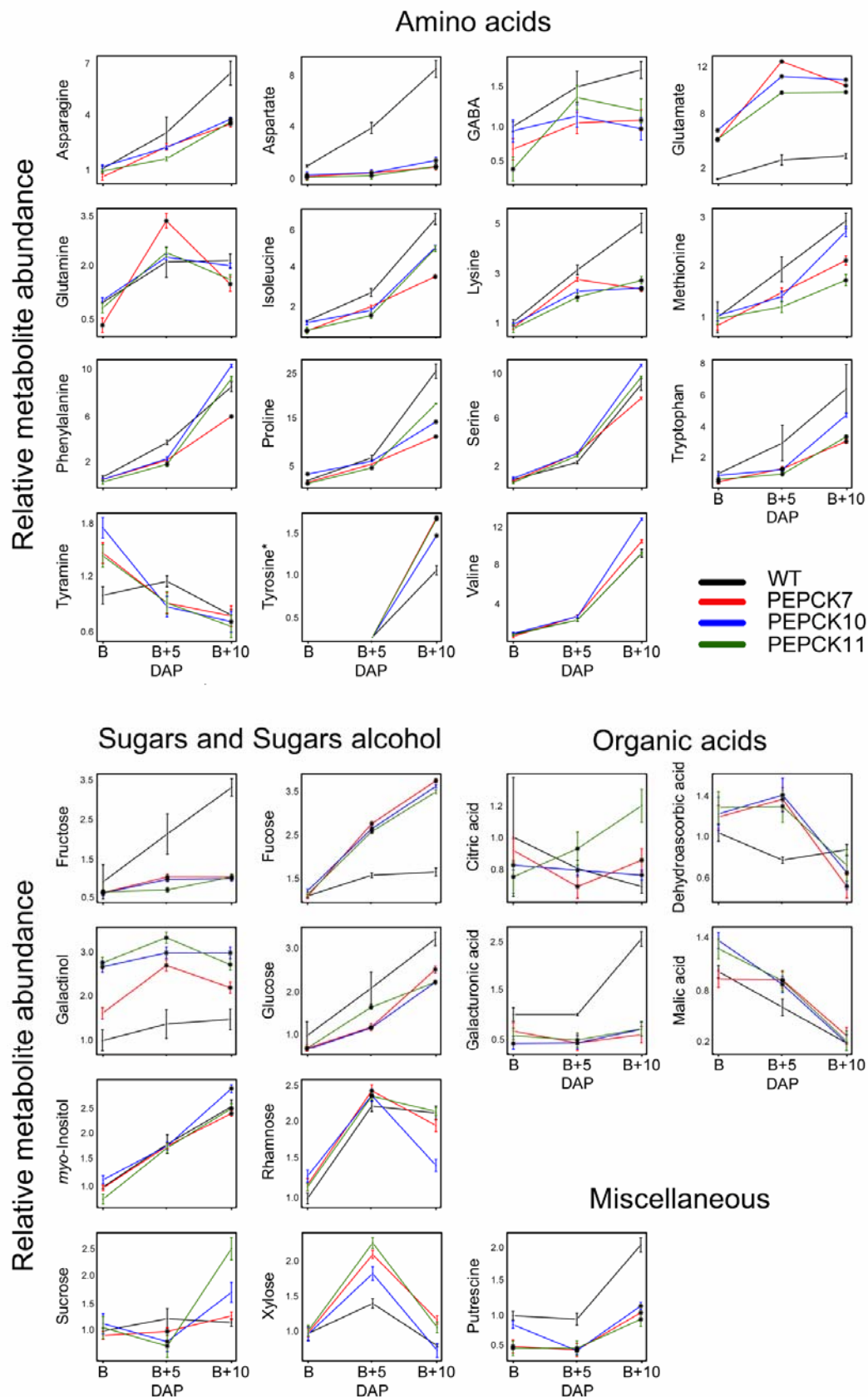


Figure 3. Primary metabolite levels in the receptacle of WT and PEPCK lines at three ripening stages (B; B+5 DAP; B+10 DAP). Data are normalized to the mean value of WT at the B stage. Values are means SE of three replicates. Black points indicate significant differences by t test ($P < 0.05$) of the transgenic lines compared with WT at the same developmental stage.

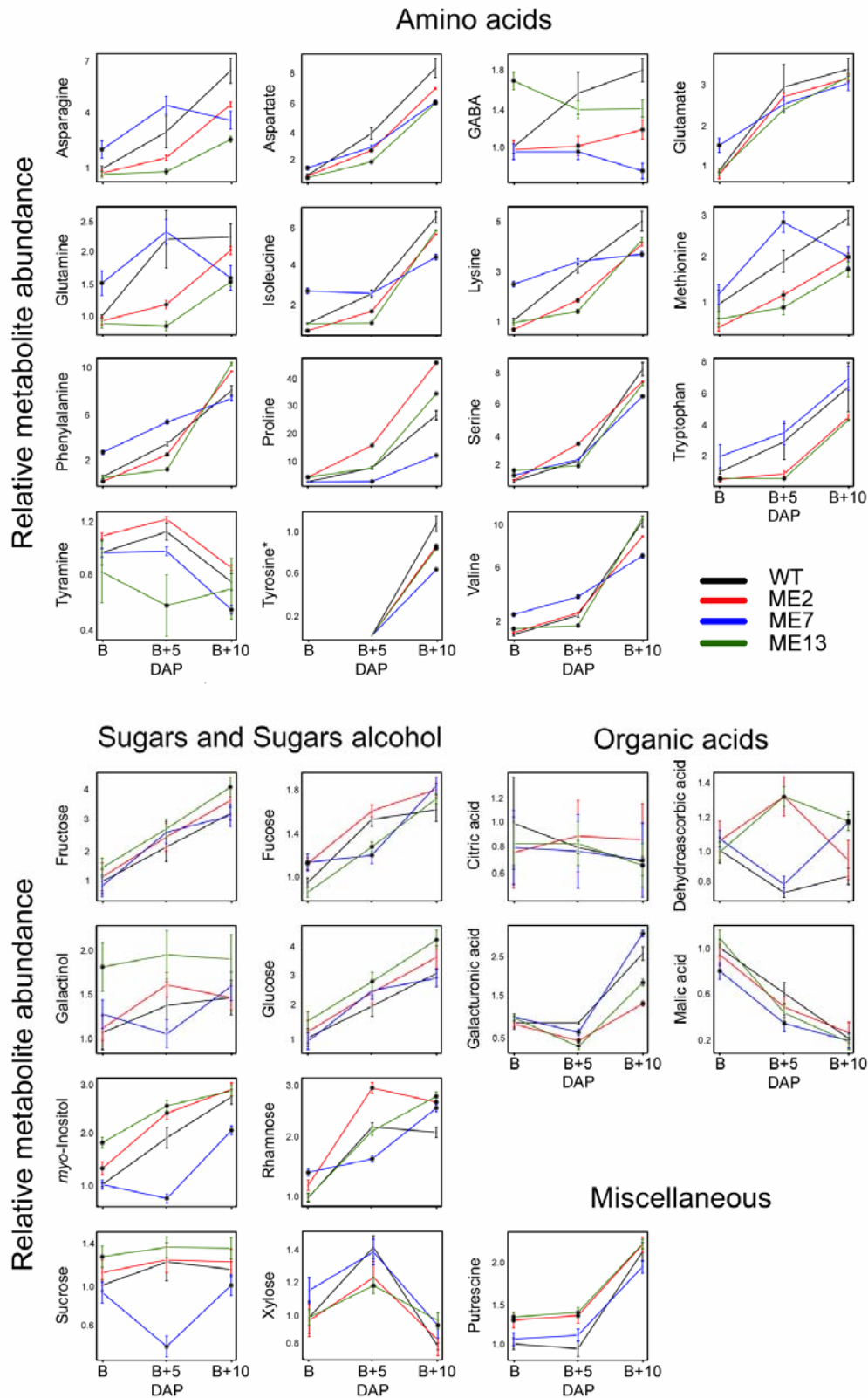


Figure 4. Primary metabolite levels in the receptacle of WT and ME lines at three ripening stages (B; B+5 DAP; B+10 DAP). Data are normalized to the mean value of WT at the B stage. Values are means SE of three replicates. Black points indicate significant differences by t test ($P < 0.05$) of the transgenic lines compared with WT at the same developmental stage.

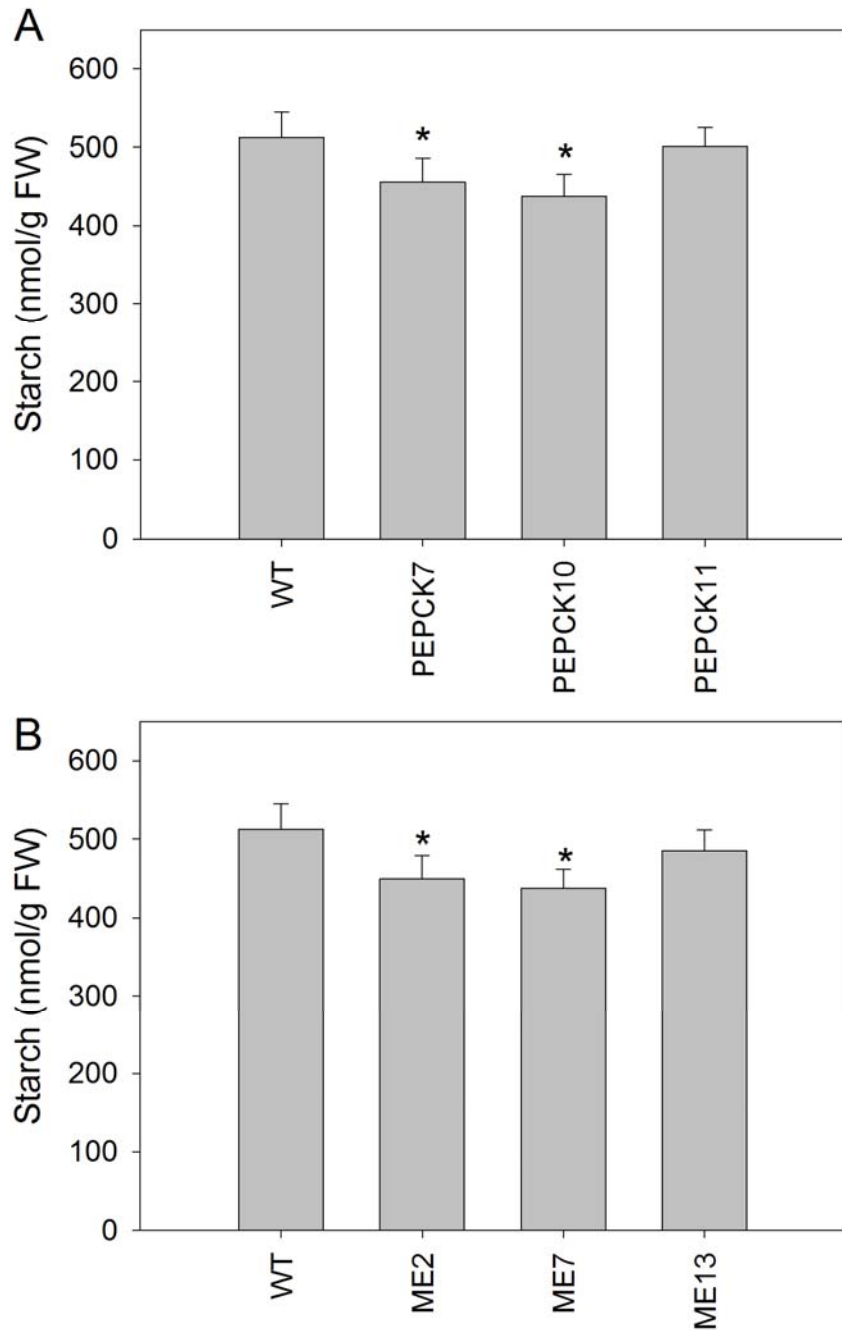


Figure 5. Starch content of PEPCK and ME lines.

(A) Starch content in the PEPCK and (B) ME lines at breaker stage. Values are presented as means \pm SE of six individual plants per line. An asterisk indicates the values that were determined by the *t* test to be significantly different ($P < 0.05$) from wild type.

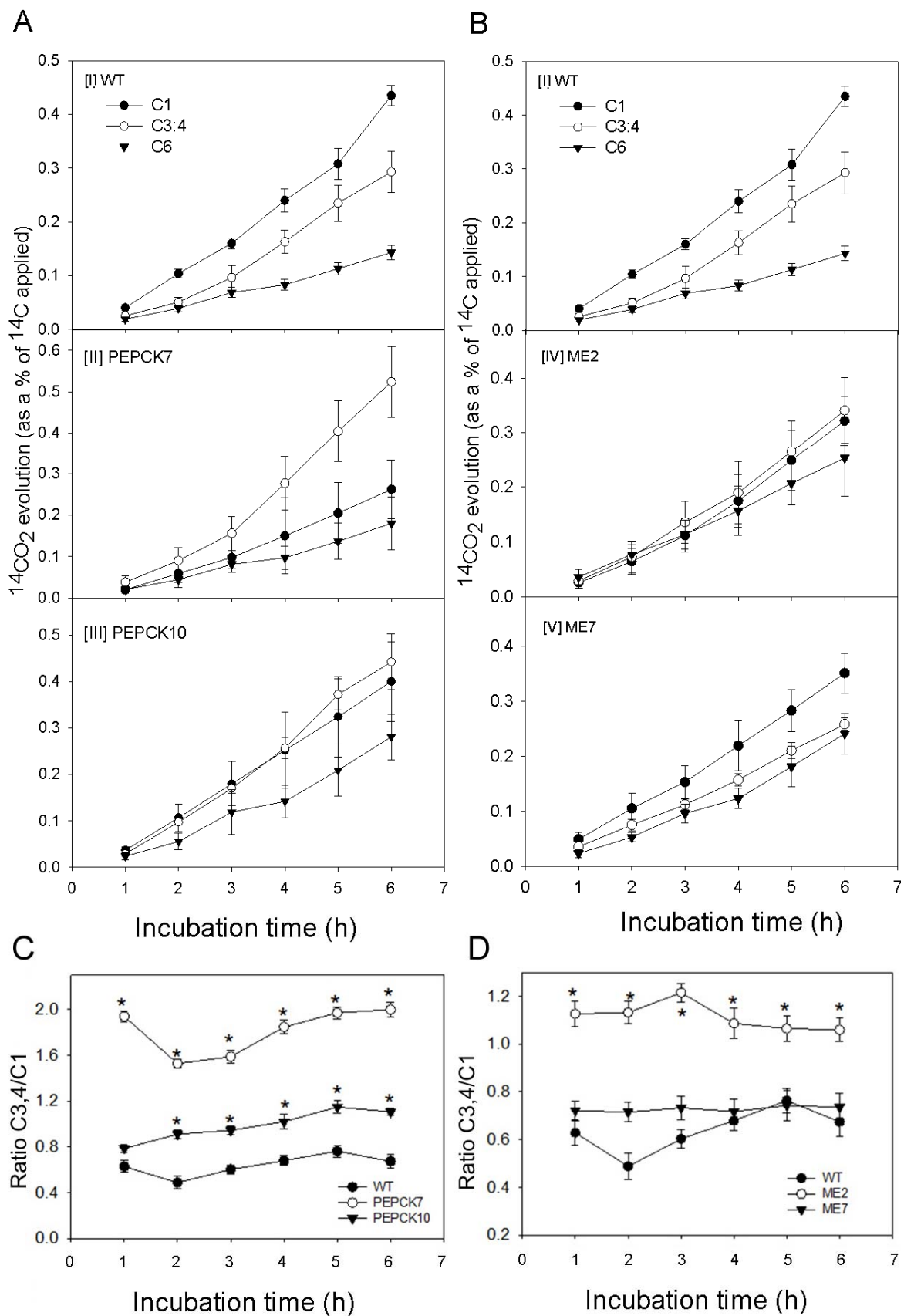


Figure 6. Respiratory parameters in Breaker + 10 DAP fruits of PEPCK and ME lines. (A, B) Evolution of ¹⁴CO₂ from breaker + 10 DAP pericarp discs of PEPCK and ME lines, respectively. (C, D) Ratio of dioxide evolution from C_{3,4}/C₁ positions of glucose in breaker +10 DAP pericarp discs of PEPCK and ME lines, respectively.

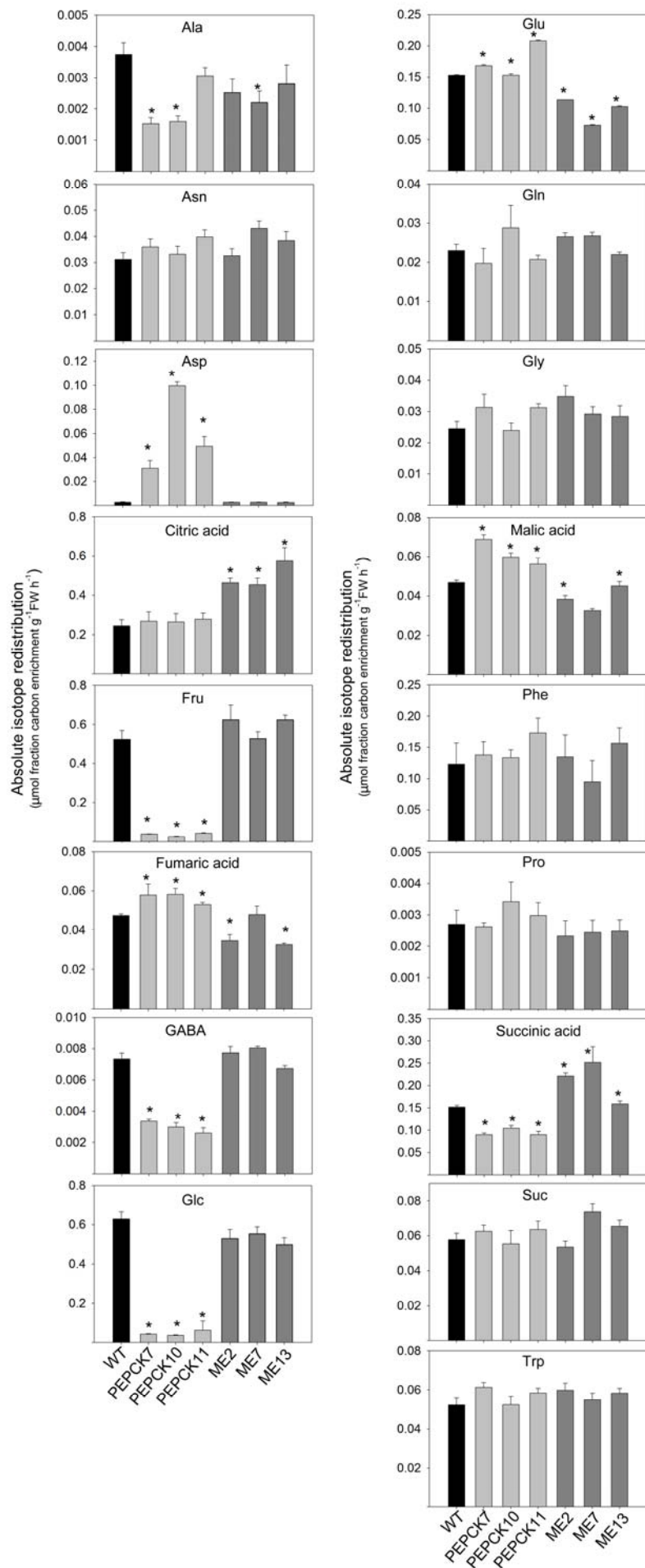


Figure 7. Redistribution of ¹³C label following incubation of transgenic lines (PEPCK and ME) and WT fruits (breaker + 10 DAP stage). The absolute isotope redistribution (μmol fraction carbon enrichment g⁻¹ FW h⁻¹) after incubation period of 6 h of [U-¹³C] Pyr. Values are means ± SE of determinations on four independent sampling; and asterisk indicates values that were determined by the Student's *t* test to be significantly different (P < 0.05) from WT.